



Contents lists available at ScienceDirect

Arabian Journal of Chemistry

journal homepage: www.ksu.edu.sa

Original article

Carboxylic acid functionalized para-xylene based hypercrosslinked polymer as a novel and high performance adsorbent for heavy metal removal

Parsa Rostami, Mohammad Reza Moradi, Mahyar Ashourzadeh Pordsari, Ahad Ghaemi*

School of Chemical, Petroleum and Gas Engineering, Iran University of Science and Technology, Iran



ARTICLE INFO

Keywords:

Heavy metal adsorption
Carboxylic acid functionalization
Selectivity
Response Surface Methodology

ABSTRACT

In this work, hypercrosslinked polymeric adsorbent (HCP) was synthesized from para-Xylene precursor through Friedel-Crafts reaction. Additionally, heavy metal adsorption experiments from a multi component system including lead, cadmium, nickel, and copper ions were conducted. To enhance lead uptake selectivity over other metallic ions, the resulting HCP sample was functionalized through carboxylic acid incorporation into the HCP adsorbent skeleton. The adsorption process modeling was carried out by using Central Composite Design-Response Surface Methodology technique. In addition, the adsorption capability dependency of the resulting samples to the operational condition including temperature from 25 °C to 65 °C, solution pH value from 4 to 10, and solution initial concentration from 20 mg/l to 100 mg/l was investigated. Additionally, process optimization was applied aim to maximize the lead uptake selectivity, the optimal condition including a temperature of 31.8 °C, pH of 5.0, and initial concentration of 82.50 mg/l were obtained for HCP sample, also the optimal condition namely a temperature of 30 °C, pH of 5.5, and initial concentration of 100 mg/l were obtained for modified HCP sample. As a result of isotherm modeling, the Hill model was obtained as the best model, additionally, thermodynamically investigation of the process resulted in spontaneously and physically adsorption of the metallic ions by HCP samples, with respect to Gibbs free energy ($\Delta G^0 < 0$) and adsorption process enthalpy ($\Delta H^0 < 20$ kJ/mol). Finally, adsorbents regeneration were evaluated and minor losses in the adsorption capacity of samples were yielded after ten cycles.

1. Introduction

Heavy metal ions define as a specific group of metals with a specific gravity value higher than 5 and molecular weight between 63.5 g/mol and 200.6 g/mol. This group of metals such as copper (Cu), iron (Fe), nickel (Ni), mercury (Hg), cobalt (Co), cadmium (Cd), etc. have high toxicity at low concentration even in ppb level (Masoumi et al., 2021). Heavy metals are stable pollutants that emote to environments through anthropogenic or natural resources. In contrast to organic pollutant, this type of pollutant is not degradable in the environment, and accumulation of these metal ions on human texture have major consequence such as neural system dysfunction, cancer, anemia, respiratory problems, skin destruction, kidney failure, etc. Thus, the heavy metal ions removing from industrial sewage is an efficient technique for the prevention of heavy metal accumulation in the environment (Masoumi et al., 2021). A series of methods have been investigated for metallic ions removal from wastewater such as electrochemical reduction (Chen et al., 2013), membrane separation (Castro-Muñoz et al., 2021), chemical

precipitation (Chen, 2018), ion exchange (Hubicki and Kołodyńska, 2012), solvent extraction (Shih et al., 2019), biological removal (Ubando, 2021), and adsorption (Masoumi et al., 2021; Wang et al., 2019; Li, 2018; Fiyadh, 2019). Among the mentioned methods the adsorption method is a favorable technique to remove metal ions from wastewater due to raw materials availability, reduction of toxic substance production, low energy consumption, and ability to adsorb the metal ions even at a low concentration (Huang, 2021). The adsorption process involves attaching liquid or gas molecules to an adsorbent's surface. Adsorption may be divided into two categories, physisorption happens when the adsorbate molecule joined to adsorbent's surface through the van der Waals interaction in contrast, chemisorption occurs when the adsorbate molecule attached to the adsorbent surface through chemical bonding (Fiyadh, 2019). Many porous solids adsorbent have been developed such as silicates (ALothman, 2012), activated carbon (Özsin et al., 2019), zeolites (Wei et al., 2015), metal organic frameworks (MOFs) (Li, 2018; Yuan, 2018), and porous organic polymers (POPs) (Wang, 2019; Mu, 2022; Cui, 2020; Konstas, 2012; Zhou, 2022; Zhu, 2014). Although some of the carbon materials such as Graphene

* Corresponding author at: School of Chemical, Petroleum and Gas Engineering, Iran University of Science and Technology, PO Box: 16846-13114, Iran.
E-mail address: aghaemi@iust.ac.ir (A. Ghaemi).

<https://doi.org/10.1016/j.arabjc.2024.105634>

Received 6 July 2023; Accepted 14 January 2024

Available online 19 January 2024

1878-5352/© 2024 The Author(s). Published by Elsevier B.V. on behalf of King Saud University. This is an open access article under the CC BY license (<http://creativecommons.org/licenses/by/4.0/>).

Nomenclature			
C_e	Equilibrium concentration	ΔG	Gibbs free energy change
k_L	Langmuir model constant (L/mg)	DCE	Dichloro Ethane
k_F	Freundlich model constant ($\text{mg}^{1-1/n} \cdot \text{L}^{1/n}/\text{g}$)	FDA	Formaldehyde Dimethyl Acetal
k_h	Hill model constant (L/mg)	HCP	Hyper Cross-linked Polymer
K_d	Distribution factor	POPs	Porous Organic Polymers
m	mass of adsorbent(g)	MOFs	Metal Organic Frameworks
V	Solution volume (ml)	MPV	micro pore volume
q	adsorption capacity (mg/g)	MPA	micro pore area
q_e	equilibrium adsorption capacity (mg/g)	APW	average pore width
q_m	maximum adsorption capacity (mg/g)	EDS	Energy Dispersive X-ray Spectroscopy
R^2	correlation coefficient	FTIR	Fourier transform infrared
AARD	Absolute Average Relative Deviation (%)	PSD	pore size distribution
T	temperature ($^{\circ}\text{C}$)	BET	Brunauer Emmett Teller
w	mass of adsorbent (g)	ICP-OES	Inductively Coupled Plasma- Optical Emission Spectrometry
ΔH	Enthalpy change	RSM	Response Surface Methodology
ΔS	Entropy change	CCD	Central Composite Design

oxide (GO) are considered as a good candidate for pollutant adsorption purposes due to its oxygen-containing functional groups rich nature, but some disadvantages of this material such as significant dispersibility poses difficulties in water treatment, which complicates the separation process and raises worries about environmental pollution. Moreover, the presence of agglomeration, resulting from π - π stacking interactions, decreases the surface area, hence restricting its efficacy in adsorption applications (Liu, 2023). Therefore, developing a novel porous materials with a large surface area and tailored surface chemistry is vital to tackle the mentioned challenges that porous adsorbents are faced with them.

Hyper cross linked polymers (HCPs) are considered as an important subgroup of the POPs with an amorphous structure which can be formed by cross linking of aromatic rings through Friedel-Crafts alkylation reaction in the presence of an external cross linker and a Lewis acid catalyst (Moradi, CO2). Additionally, some morphological characteristics of the HCPs including surface area, pore volume, and adsorption properties are adjustable by making changes in cross linker and catalyst amount during the synthesis process (Ramezanipour Penchah et al., 2019). Due to the HCP's unique characteristics such as low density, high surface area, tunable pore sizes, scale-up, thermal stability, chemical and mechanical resistance, and low heat adsorption, this materials have been known as promising candidate for practical application of heavy metal removing from wastewaters (Masoumi et al., 2021). Despite the good morphological properties of the HCPs which causes high heavy metals adsorption capability, the presence of aromatic rings in the adsorbent structure result in cation- π interaction between heavy metal ions and the adsorbent surface that improve metal adsorption capacity of the HCPs through physisorption mechanism. Additionally, the incorporation of some functional moieties like amine group, carboxyl group, hydroxyl group, and sulfhydryl group enhance HCPs adsorbent metal ions capture capability through making changes in HCPs surface potential heterogeneity or acting as an active ligand site (Wang et al., 2019; Li, 2015).

Based on the literature review, many studies on heavy metal adsorption have investigated the heavy metal uptake capability of the polymeric adsorbent in a single component system, but it should be considered industrial wastewater contain various metal ions. In the multi component system, an electrostatic field is created by the interaction among charged ions, which will further affect how the heavy metal ions approach the sorbent. Therefore, considering the competition among the different cations for occupying surface cavities, it is important to look into how metal ions are adsorbed when other metal ions are present (Masoumi et al., 2021). In recent years, investigations on the heavy metals uptake from multi component systems by using polymeric adsorbents have been

increased gradually. For example, Ebrahimpour et al. synthesized a novel hydrogel polymer for effective uptake of Hg^{2+} and Pb^{2+} ions from wastewater (Ebrahimpour and Kazemi, 2023). Verma et al. provided a trifunctional β - cyclodextrin - ethylenediaminetetraacetic acid - chitosan polymer aim to adsorption of mercury (Hg^{2+}) and cadmium (Cd^{2+}) cations from aqueous media (Verma, 2022). A hybrid polymer, synthesized via in situ polymerization of pyromellitic acid dianhydride and N-(3-(trimethoxysilyl) propylene ethylene diamine, followed by functionalization with toluene 2, 4-diisocyanate, is proposed as a sorbent for removal of the Co^{2+} , Pb^{2+} , and Cr^{3+} ions, by A. M. Aldawsari et al (Aldawsari, 2022). Wang et al. provided a polymer called Zn-CP, which shows good efficiency in uptake of Fe^{3+} ions from water (Wang, 2022). Y. Sun et al. prepared dual-functional chitosan and investigated the adsorption of the nickel (Ni^{2+}) ion from waste water (Sun, 2020). Badruddoza, A.Z.M., et al. provided a novel polymer modified whit Fe_3O_4 nanoparticles, for the selective adsorption of Pb^{2+} , Cd^{2+} , and Ni^{2+} ions (Badruddoza, 2013). Ge, F., et al. studied the uptake of the Pb^{2+} , Cd^{2+} , Zn^{2+} , and Cu^{2+} ions from waste water by utilizing Fe_3O_4 nanoparticles modified copolymer (Ge et al., 2012).

In this work, a hyper cross-linked polymeric adsorbent was synthesized based on xylene monomer and heavy metal ions adsorption experiments were conducted in a multi component system including Nickel, Cadmium, Lead, and Copper ions solution. To enhance the xylene based HCP sample hydrophilicity, adsorption capacity, and selectivity, the carboxyl group ($-\text{COOH}$) incorporation to the polymer network was done and the adsorption tests were performed again at similar condition. To study the morphological properties of adsorbents and the success of carboxyl functionalization to xylene based HCP, the BET, EDX, and FTIR analysis were performed and the results were reported. Additionally, to investigate the impact of effective adsorption factors such as temperature, initial concentration, and pH on the competitive uptake behavior of heavy metal ions on adsorbent surfaces, the design of experiment (DOE) was carried out aimed to optimize mentioned parameters and present the quadratic predictive models for all of the metallic ions adsorption efficiency at optimum condition. Finally, the metallic ions adsorption mechanisms by both types of adsorbents were evaluated using isotherm and thermodynamic modeling of the adsorption process and model parameters were reported.

2. Material and methods

2.1. Chemicals

The industrial grade of para-xylene was prepared from Dr. Mojallali

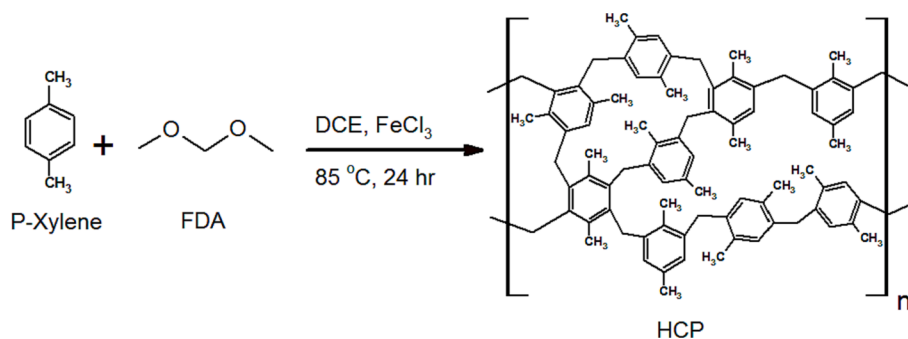


Fig. 1. Para xylene based HCP sample synthesis procedure.

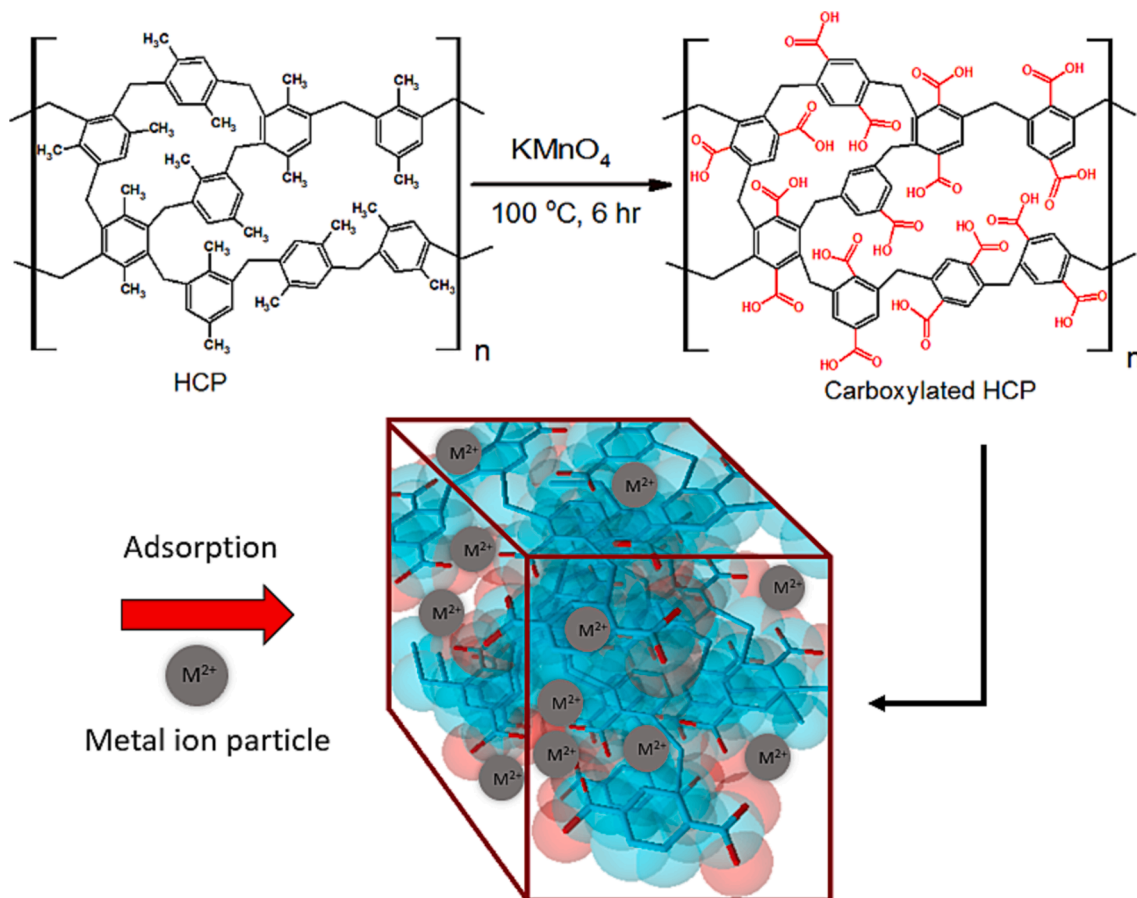


Fig. 2. Carboxylic acid modification procedure of the HCP sample.

Table 1

Levels of the operating factors in RSM modeling.

Parameter	Name	Unit	Coded value ($\alpha = 2$)				
			-2	-1	0	1	2
A	Temperature	$^\circ\text{C}$	25	35	45	55	65
B	pH	-	4	5.5	7	8.5	10
C	Initial concentration	mg/l	20	40	60	80	100

industrial chemical complex company. In addition, anhydrous iron (III) chloride, potassium permanganate (KMnO_4), 1,2-dichloro ethane (DCE), formaldehyde dimethyl acetal (FDA), and ethanol were prepared from Merck company. During the xylene based HCP preparation and post modification, deionized water and distilled water were used for washing purposes. Also lead nitrate ($\text{Pb}(\text{NO}_3)_2$), cadmium nitrate

($\text{Cd}(\text{NO}_3)_2 \cdot 4\text{H}_2\text{O}$), nickel nitrate ($\text{Ni}(\text{NO}_3)_2 \cdot 6\text{H}_2\text{O}$), and copper nitrate ($\text{Cu}(\text{NO}_3)_2 \cdot 3\text{H}_2\text{O}$) were purchased from Merck company. The aforementioned raw materials were applied without further purification.

2.2. Para-xylene based HCP synthesis

In general, the hyper cross linked polymeric adsorbent (HCP) is synthesized through Friedel-Crafts alkylation reaction by using an external cross linker agent to form covalent bonds between aromatic ring of the monomers. In this work, similar to the technique reported by Li et al. (Li, 2011), the HCP adsorbent was synthesized based on para-xylene as monomer. To obtain the highest specific surface area and maximum heavy metal ions adsorption capability, the synthesis parameters such as synthesis time and monomer to cross linker ratio were adjusted in an optimal condition that was presented by Kim et al (Kim,

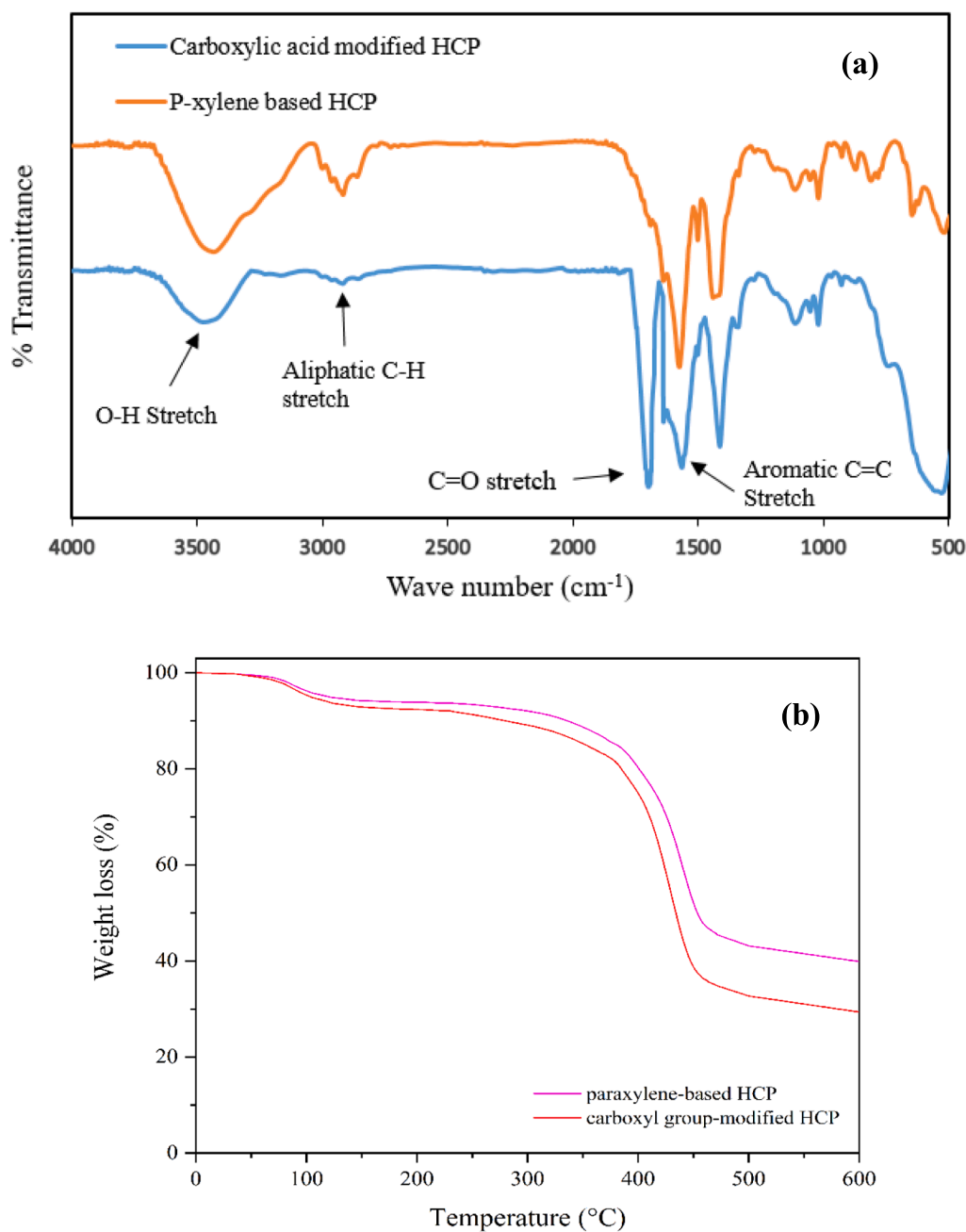


Fig. 3. a) FT-IR spectra of the HCP and carboxylated HCP sample, b) TGA analysis results of the both sample.

2020). Typically, para-xylene (0.02 mol), formaldehyde dimethyl acetal (0.04 mol), and dichloro ethane (40 ml) were poured into a three-Neck round bottom flask, then the flask contents were agitated at 25 $^{\circ}\text{C}$ for 1 h in the argon atmosphere. Then the anhydrous iron (III) chloride powder (0.04 mol) was charged to the flask and the mixture was blended at 45 $^{\circ}\text{C}$ for 4 h. Next, the mixture temperature was increased to 85 $^{\circ}\text{C}$, followed by mixing in the reflux condition for 24 h. Next, the obtained porous polymeric adsorbent was filtrated and aimed to remove the solvent and excess reactants, the resulting polymer was washed several times with distilled water and ethanol for 20 h by soxhlet extractor apparatus. Finally, the purified HCP adsorbent dried at 160 $^{\circ}\text{C}$ for 15 h. The para-xylene based HCP synthesis method is shown in Fig. 1.

2.3. Para-xylene based HCP's surface modification

The presence of electron-withdrawing groups such as amine or

amide group, phenol group, or carboxylic acid group in the HCP adsorbent's skeleton enhances the HCPs adsorbent heavy metal ions uptake capability by improving the adsorbent's surface heterogeneity. In addition, the presence of lone pair electrons on electron donor atoms such as oxygen, nitrogen, or sulfur act as ligand active sites and improve the selectivity of the HCP in the selective adsorption of cations. In this work, surface modification of xylene based HCP sample was done by incorporation of carboxylic acid group ($-\text{COOH}$) to the HCP adsorbent network. Carboxylic acid modification of the HCP sample was carried out through the oxidation of the xylene's methyl group ($-\text{CH}_3$) by utilizing a strong oxidizing agent namely potassium permanganate (KMnO_4). In a typical procedure, the HCP adsorbent (4 g) and distilled water (250 ml) were charged to a three-neck flask, and the contents were heated at 100 $^{\circ}\text{C}$ in the reflux conditions until the mixture reached to the boiling point. Then, potassium permanganate (KMnO_4) was added to the mixture in three stages. First, KMnO_4 (8 g) was charged to the flask

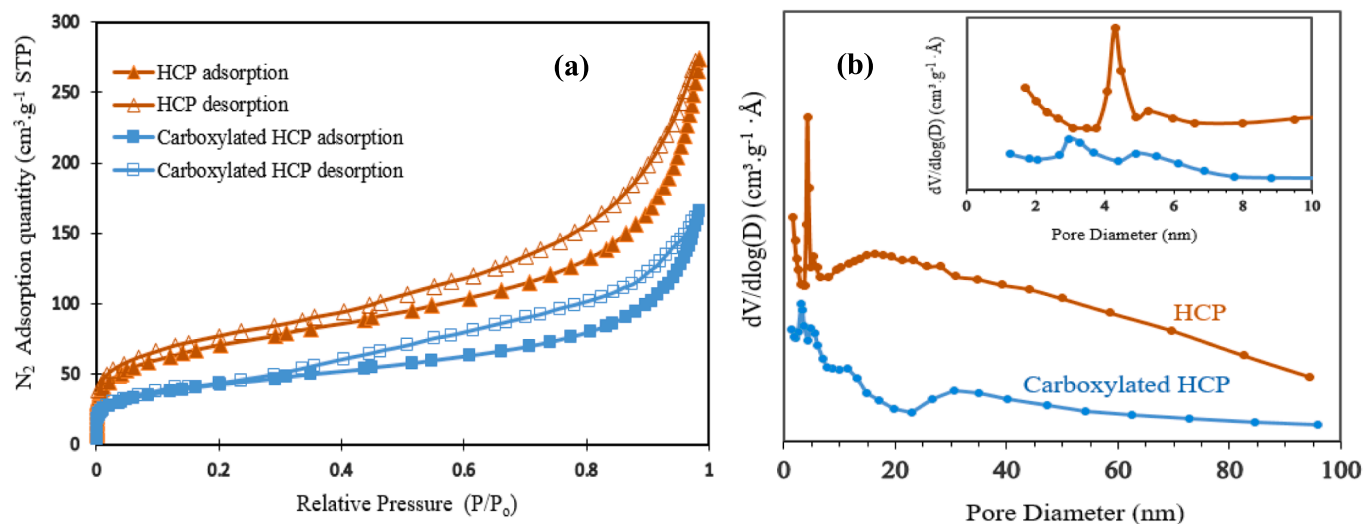


Fig. 4. a) Nitrogen adsorption–desorption isotherms of the samples, b) Pore size distribution plots of the HCP samples.

Table 2

Porous properties of the HCP and the modified HCP sample.

Sample	S_{BET}^a (m^2/g)	MPV^b (cm^3/g)	MPA^c (m^2/g)	PV^d (cm^3/g)	APW^e (nm)
Xylene based HCP	237.73	0.074	14.85	0.396	6.283
Carboxylic acid modified HCP	153.43	0.108	26.61	0.267	5.346

^a Specific surface area (based on BET model).

^b Micropore volume.

^c Micropore area.

^d Total pore volume.

^e Average pore width (based on 4 V/A equation).

followed by stirring under reflux condition and solution's boiling point for 2 h. Next, KMnO_4 (4 g) was added to the mixture and the reaction continued for 2 h. Finally, KMnO_4 (4 g) was added to the mixture in the third stage and the mixture was kept for 3 h at the boiling point of the mixture. Next, the flask contents were cooled down and the flask contents were washed with distilled water several times. Then, aimed to remove the remained manganese ions and the carboxylic acid groups recovery, the resulting modified HCP was washed with 500 ml of 0.01 M hydrochloric acid (Vogel and Furniss, 1978). Finally, the obtained modified HCP was dried at 160°C for 15 h in a vacuum oven. The xylene based HCP carboxylic acid functionalization procedure is shown in Fig. 2.

2.4. Adsorbent characterization

The p-xylene based HCP and the carboxylic acid modified HCP's elemental composition were characterized by energy dispersive X-ray spectroscopy (EDS) analysis using Philips- $\times 130$ instrument, also X-ray photoelectron spectroscopy (XPS) technique was applied by an Al $K\alpha$ source (XPS spectrometer Kratos AXIS Supra) device. The adsorbents morphological properties were characterized by nitrogen adsorption–desorption method at 77.3 K using ASAP 2020 M analyzer. To characterize the adsorbents structural properties and functional groups, FTIR analysis was performed by using PerkinElmer FTIR spectrometer instrument. Thermal stability of the samples were evaluated using thermogravimetric analysis (TGA) under an N_2 atmosphere (TGA, model 2960, Universal V 2.4F TA instrument). To measure the concentration of the metallic cations in liquid samples, the inductively coupled plasma-optical emission spectrometry (ICP-OES) analysis was carried out by (ICP-OES, series 5800) instrument.

2.5. Adsorption experiments and selectivity

To perform the heavy metal adsorption experiments, the heavy metal ions contain solutions with different initial concentration including 20, 40, 60, 80, and 100 mg/l were prepared from stock solution with a concentration of 200 mg/l. Next, the resulting solution (150 ml) was charged to a flask, then the sample's pH value was adjusted to a desired value by using 0.05 M NaOH solution or 0.05 M HCL solution, also the oil bath temperature was adjusted. The adsorption process was started

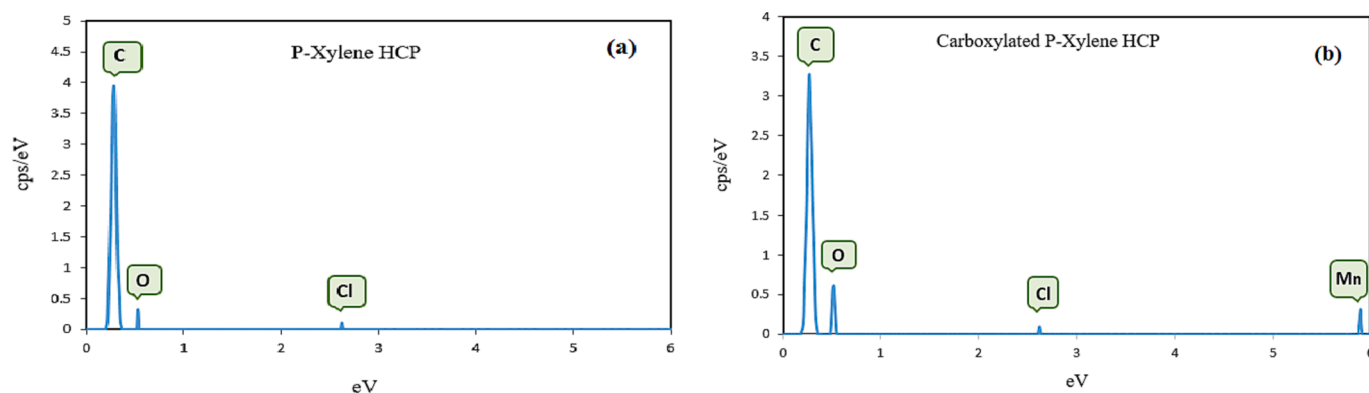


Fig. 5. EDS pattern of the a) xylene based HCP, b) modified HCP sample.

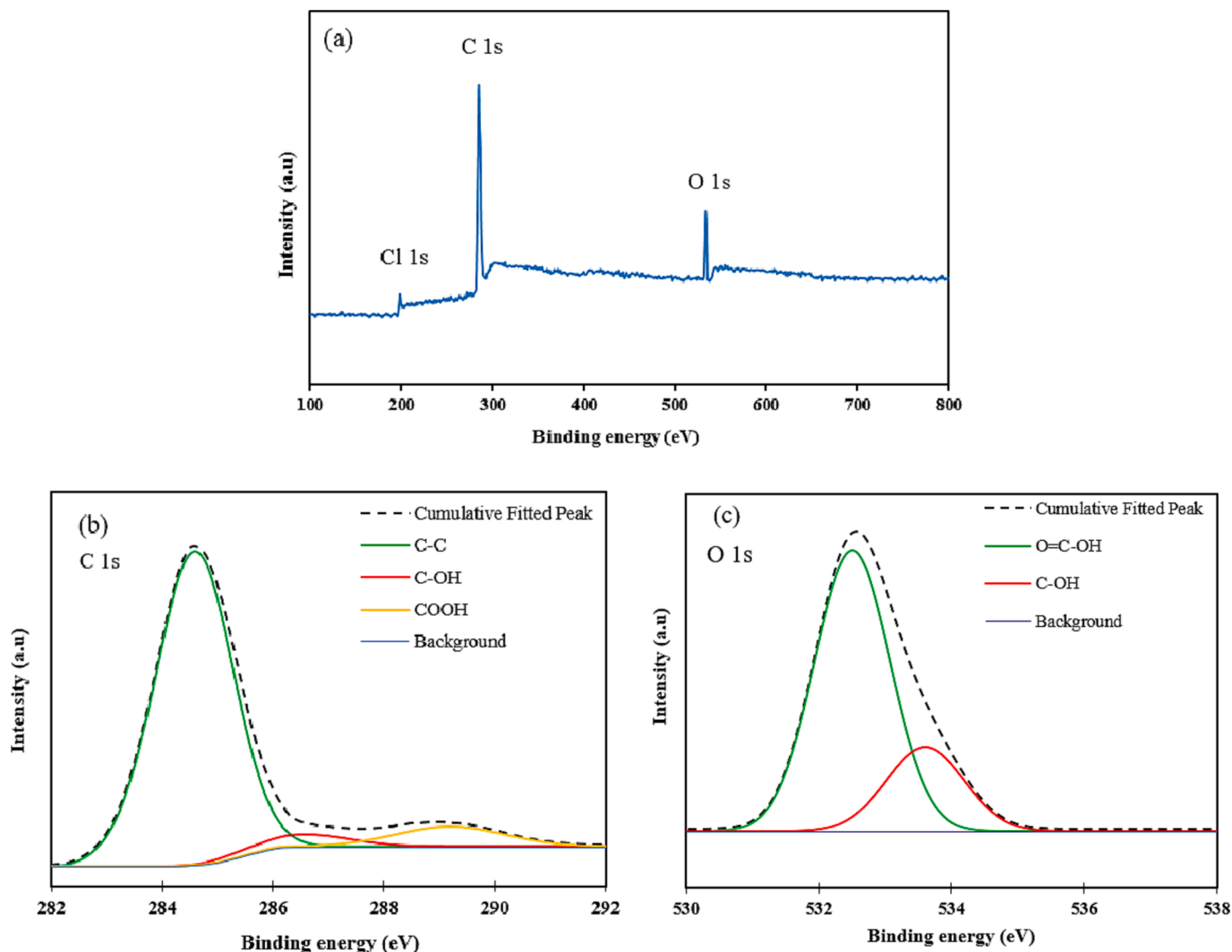


Fig. 6. The carboxylic acid modified HCP's XPS results, a) survey scan spectra, b) High resolution C 1s spectra, and c) High resolution O 1s spectra.

by the addition of 0.1 gr adsorbent powder and stirring the flask contents at 1000 rpm. The adsorption process continued for 4 h to reach an equilibrium state, after 4 h the flask contents were filtrated and the quantity of the heavy metal ions in the residual solution was measured using ICP-OES analysis. The differences between the initial concentration and final concentration of the metallic ions refer to the quantity of adsorbed heavy metal ions. The metal ions equilibrium adsorption capacity (q_e), removal efficiency (RE%), distribution factor value (D), and selectivity value (S) in a multi component adsorption system can be calculated by using equations (1–4), respectively (Wang and Liu, 2014).

$$q_e = \frac{(C_0 - C_e)V}{m} \quad (1)$$

$$RE = \frac{C_0 - C_e}{C_0} \times 100 \quad (2)$$

$$D = \frac{q_e}{C_e} \quad (3)$$

$$S\left(\frac{M_I}{M_{II}}\right) = \frac{D_I}{D_{II}} \quad (4)$$

Where C_0 , C_e , m , V , M_I , and M_{II} refer to the cation's initial concentration, final concentration, weight of adsorbent, volume of the solution, metallic cation I, and metallic cation II, respectively.

2.6. Design of experiment

Design of experiment (DOE) is a useful statistical tool, which can correlate the independent input parameters to system output (response). Applying DOE has some advantages including identifying the most effective parameters, elimination of the excessive cost of experiment, and optimization of process regarding achieving the highest yield (Bashir et al., 2010). Response Surface Methodology (RSM) is one of the applicable approaches of the DOE, which can make a relationship between inputs and output by correlating the empirical data on a quadratic function that is represented in equation (5). The resulting model's accuracy and significance assessment can be investigated by analysis of variance (ANOVA) and other statistical criterions such as correlation coefficient (R^2) and Average Absolute Relative Deviation (AARD %) values which can be calculated using equation (6) and equation (7), respectively (Zaferani et al., 2019).

$$Y = \beta_0 + \sum_{i=1}^k \beta_i x_i + \sum_{i=1}^k \beta_{ii} x_i^2 + \sum_{\substack{i=1 \\ j>i}}^k \beta_{ij} x_i x_j \quad (5)$$

$$R^2 = \frac{\sum_{i=1}^n (Y_{predict} - Y_{actual})^2}{\sum_{i=1}^n (Y_{predict} - Y_{Mean})^2} \quad (6)$$

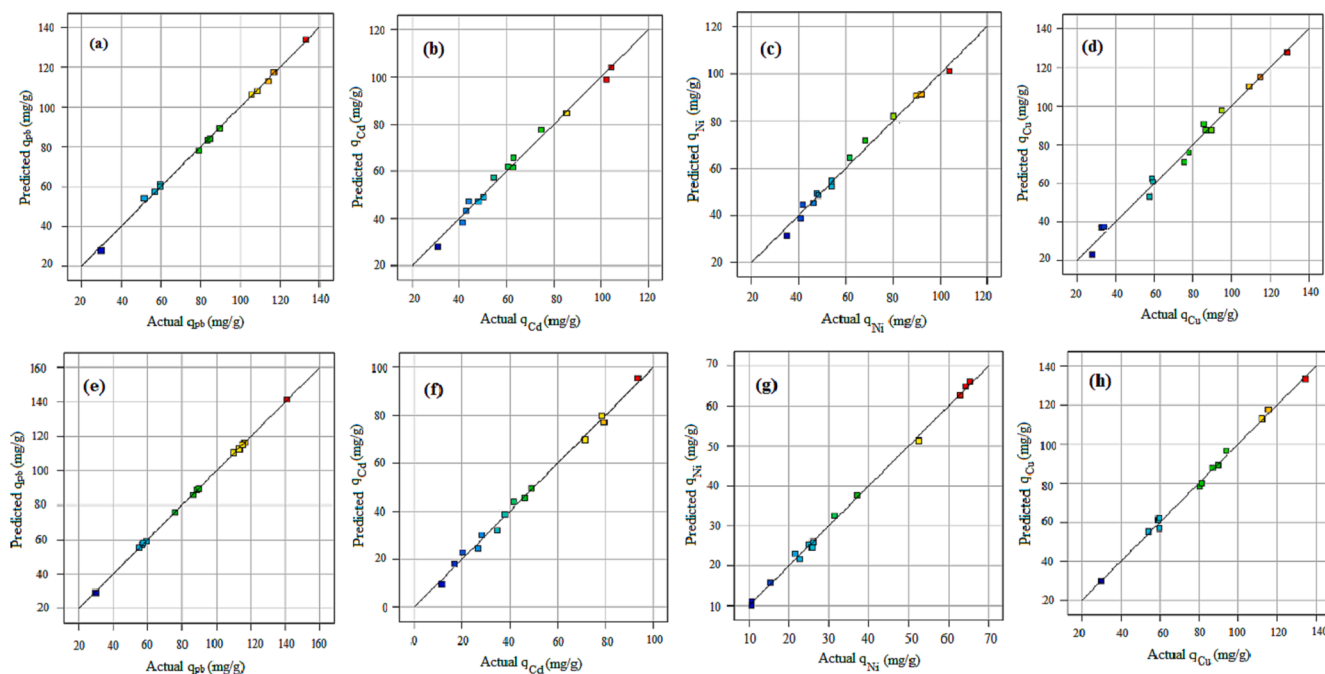


Fig. 7. Predicted versus actual heavy metal adsorption data utilizing HCP sample for a) lead, b) cadmium, c) nickel, d) copper, and utilizing carboxylic acid modified for e) lead, f) cadmium, g) nickel, h) copper.

$$AARD\% = 100 \times \frac{1}{n} \times \sum_{i=1}^n \frac{|Y_i^{act} - Y_i^{pred}|}{Y_i^{act}} \quad (7)$$

Where x_i , x_j , and Y refers to the input parameter i value, input parameter j value, and predicted response value, respectively. Also the terms of the β_0 , β_i , β_{ii} , β_{ij} , and k defines as the function's coefficients which refer to constant coefficient, linear effect, quadratic effect, the interaction term between input parameters, and the number of input variables, respectively (Ramezanipour Penchah et al., 2019). In this work, design of experiment of the metallic ions adsorption process was performed using Design Expert software v.11 and the effective parameters including adsorption process temperature (X_1), the solution pH value (X_2), and initial concentration of the metallic cation contain solution (X_3) were considered as input parameters, also the model responses were defined as adsorption capacity of the lead ion (Y_1), cadmium ion (Y_2), nickel ion (Y_3), and copper ion (Y_4). The input parameters symbol, unit, coded values, maximum value, and minimum value were summarized in Table 1. By reviewing the literatures, it can be noticed that the heavy metals adsorption are investigated in the pH value within 4–10, due to severe corrosion problems in the pH lower than 4 and precipitation of the metallic ions in the pH higher than 10. Also, the temperature of the industrial waste waters rarely exceeds from 60 °C and usually are near to the ambient temperature. Moreover, the initial concentration for the drinking water treatment usually is lower than 100 mg/l, therefore, in this study the range of temperature, pH, and initial concentration were selected within 25–65 °C, 4–10, and 20–100 mg/l, respectively.

2.7. Isotherm modeling

To study the heavy metal adsorption behavior of the unmodified/modified HCP samples with respect to competitive adsorption of the metallic ions in a multi component system, isotherm modeling was conducted aim to investigate the adsorbate-adsorbent interactions. To correlate the equilibrium uptake capacity to the equilibrium concentration of metallic ions in the solution, five isotherm models including Langmuir, Freundlich, Hill, Dubinin-Radushkevich (D-R), and Temkin models which are represented by equations (8–12), were utilized (Masoumi et al., 2021).

$$\text{Langmuir : } q_e = \frac{q_m K_L C_e}{1 + K_L C_e} \quad (8)$$

$$\text{Freundlich : } q_e = K_F C_e^{1/n_f} \quad (9)$$

$$\text{Hill : } q_e = \frac{q_m C_e^{n_h}}{K_h + C_e^{n_h}} \quad (10)$$

$$\text{Temkin : } q_e = BLnA_T + BLnC_e, \quad B = \left(\frac{RT}{b_T}\right) \quad (11)$$

$$\text{D - R : } q_e = q_m \exp(-\lambda \omega^2), \quad \omega = RT\left(1 + \frac{1}{C}\right), \quad E = \left(\frac{1}{\sqrt{2\lambda}}\right) \quad (12)$$

The quantities q_e (mg/g) and q_m (mg/g) refer to the equilibrium uptake capacity and maximum uptake capacity, respectively. The concentration at the equilibrium state is denoted by C_e (mg/L). The Freundlich model constants are represented by K_F ($\text{mg}_i^{1-1/n_f} \cdot \text{L}_i^{1/n_f} / \text{g}$) and n_f , while the Langmuir model constant is K_L (L/mg). The Hill model constants are given by K_h (L/mg) and n_h . The parameter of λ in the Dubinin-Radushkevich model refers to the constant ($\text{mol}^2 \cdot \text{J}^{-1}$) and the terms ω , and E represent the Polanyi potential ($\text{J} \cdot \text{mol}^{-1}$), and adsorption free energy, respectively. Also in the Temkin isotherm model, the first virial coefficient is represented by term B ($B = \left(\frac{RT}{b_T}\right)$, $b_T = (\text{J} \cdot \text{mol}^{-1})$), while the term A_T ($\text{L} \cdot \text{mol}^{-1}$) is a constant (Mashhadimoslem, 2021).

2.8. Adsorption process kinetics

The adsorption mechanism and the adsorbent's efficacy in removing metal ions have been investigated using kinetic models. Experimental adsorption data were fitted using two kinetic models: pseudo-first-order and pseudo-second-order, represented by equation (13) and equation (14), respectively (Masoumi et al., 2021).

$$q_t = q_e (1 - e^{-k_1 t}) \quad (13)$$

$$q_t = (q_e^2 k_2 t) / (1 + q_e k_2 t) \quad (14)$$

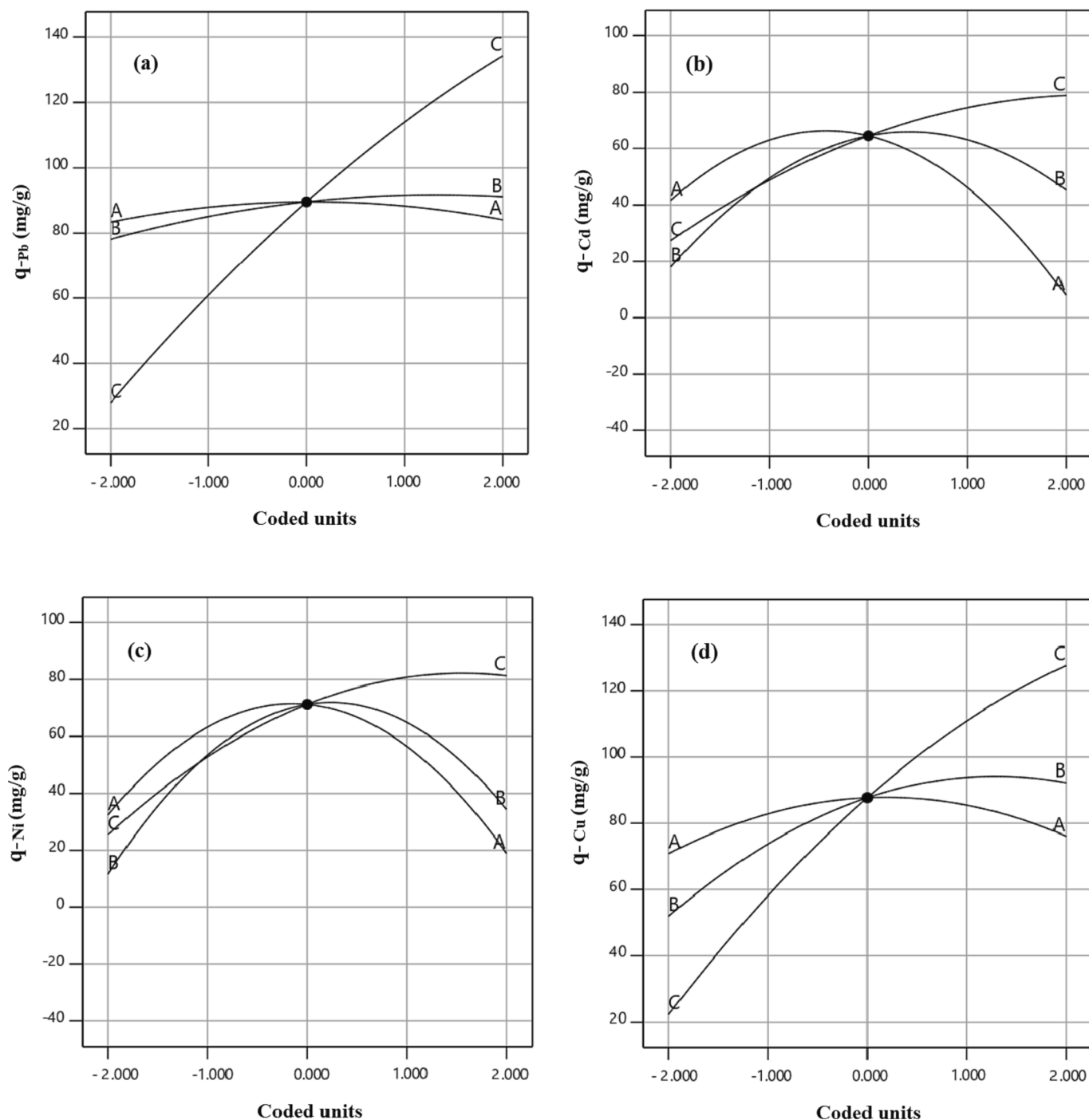


Fig. 8. Perturbation plots of the heavy metal uptake by xylene based HCP a) lead, b) cadmium, c) nickel, d) copper.

Where k_1 (min^{-1}), and k_2 ($\text{g} \cdot \text{mg}^{-1} \cdot \text{min}^{-1}$), refer to the pseudo-first-order model's rate constant, and pseudo-second-order model's rate constant, respectively. Also, the terms q_t and q_e represent the adsorption capacity at the time of t , and at the equilibrium state.

3. Result and discussion

3.1. Adsorbents characterization

The FTIR spectrum of the adsorbents in the wave number range of 500–4000 cm^{-1} are illustrated in Fig. 3.a. Based on the FTIR results, the peak at 2912 cm^{-1} is related to aliphatic C–H stretch of methylene

group which was formed through cross linking of xylene molecules, the peak at 1495 cm^{-1} corresponds to aromatic C=C stretches of xylene ring molecules. In the modified HCP FTIR spectra, the peak at 1710 cm^{-1} refer to C=O stretches of the carboxylic acid group, this peak proves the successfully incorporation of carboxylic acid group to HCP sample structure. The wide peak in the range of 3200 cm^{-1} to 3600 cm^{-1} is related to the O–H bond stretch of the carboxylic acid group, also the O–H peak in the HCP sample spectra is related to the formation of hydroxyl group through hydrolysis of the methoxy group of remained formaldehyde dimethyl acetal molecules (Kim, 2020). Thermogravimetric analysis results for both polymeric samples are presented in Fig. 3.b. According to this figure, at temperatures ranging between 80 and 100 $^{\circ}\text{C}$, a slight reduction (about 5 %) in the content of both

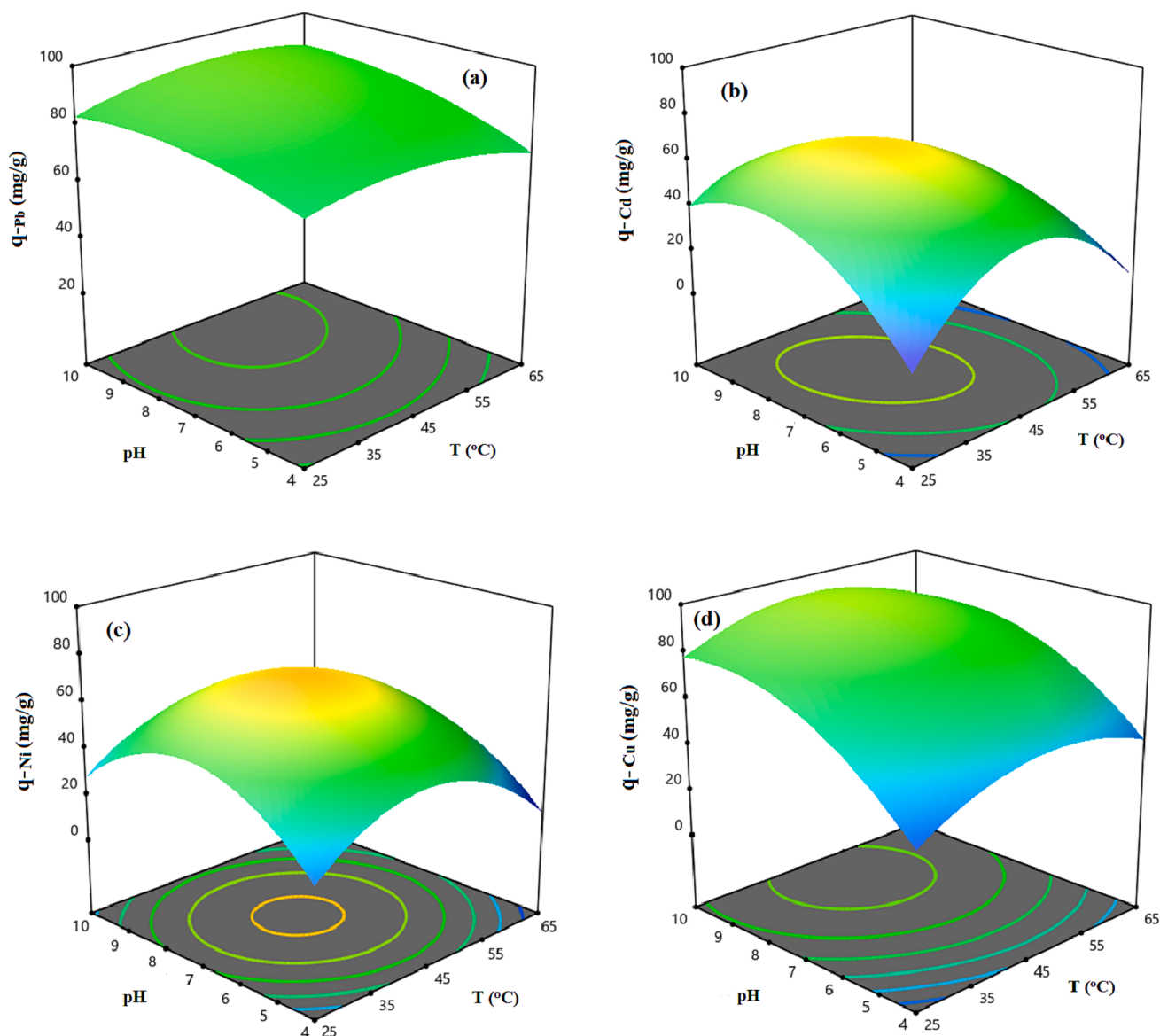


Fig. 9. 3D response surfaces representing the HCP adsorbent's uptake capacity dependency to the pH and temperature at initial concentration of 60 mg/l for a) Lead, b) Cadmium, c) Nickel, d) Copper.

adsorbents was observed, which could be related to the solvent or water evaporation. Rapidly decomposition of the samples between 370 and 470 °C may be attributed to the destruction of C—C bonds of the crosslinking bridges which were yielded from the Friedel-Crafts reaction, also the modified HCP's more weight loss can be related to the decomposition of C—O bonds of the carboxyl group (Sel, 2015). The polymeric residues of the xylene based HCP and the modified HCP adsorbents were 39.82 wt% and 33.71 wt%, respectively, at 600 °C (Maleki et al., 2022). The porous properties of the xylene based HCP sample and the carboxylic acid functionalized HCP sample were evaluated by N₂ adsorption–desorption measuring at 77.3 K, which are illustrated in Fig. 4.a. Based on Fig. 4.a, for both type of samples the type II isotherm curve were observed based on IUPAC isotherm classification. This type of isotherm curve can be attributed to the existence of micropores and meso pores in samples structure (Huang, 2009). According to the figure, sharply Nitrogen adsorption by both samples at a relative pressure range between 0 and 0.05 can be related to the presence of micropores in the samples skeleton. Additionally, the hysteresis loop presence in the adsorption–desorption isotherm at the relative pressure between 0.2 and 0.8 refers to the presence of the mesopores in the

samples structure, also the hysteresis loop in the relative pressure more than 0.8 demonstrate the existence of the macropores and interparticle voids in both type of the adsorbents network (Kong et al., 2019). The porous properties characteristics of both porous polymers were reported in Table 2. According to the table findings, the BET surface area of the xylene based HCP and the carboxylic acid modified HCP are 237.73 m²/g and 133.43 m²/g, respectively. Based on the result, the carboxylic acid functionalization of the HCP sample reduced the specific surface area of the HCP sample dramatically, it can be attributed to the partial space filling of the pores by carboxylic acid functional group (He, 2017). Fig. 4. b depicts the pore size distribution of the samples, according to this figure the pore size peak of the HCP sample is obtained around 4.25 nm and for the carboxylic acid modified HCP sample, two pore size peaks are obtained around 2.96 nm and 5.03 nm. The findings of the pore size distribution plot have good conformity with the hysteresis loop existence in N₂ adsorption–desorption isotherms, which refer to the presence of the macro pores in the structure of the samples. Based on the Fig. 4.b, the carboxylic acid group incorporation to the HCP sample skeleton increased the micropore volume of the modified HCP, it can be concluded that incorporation of the carboxylic acid to polymer network

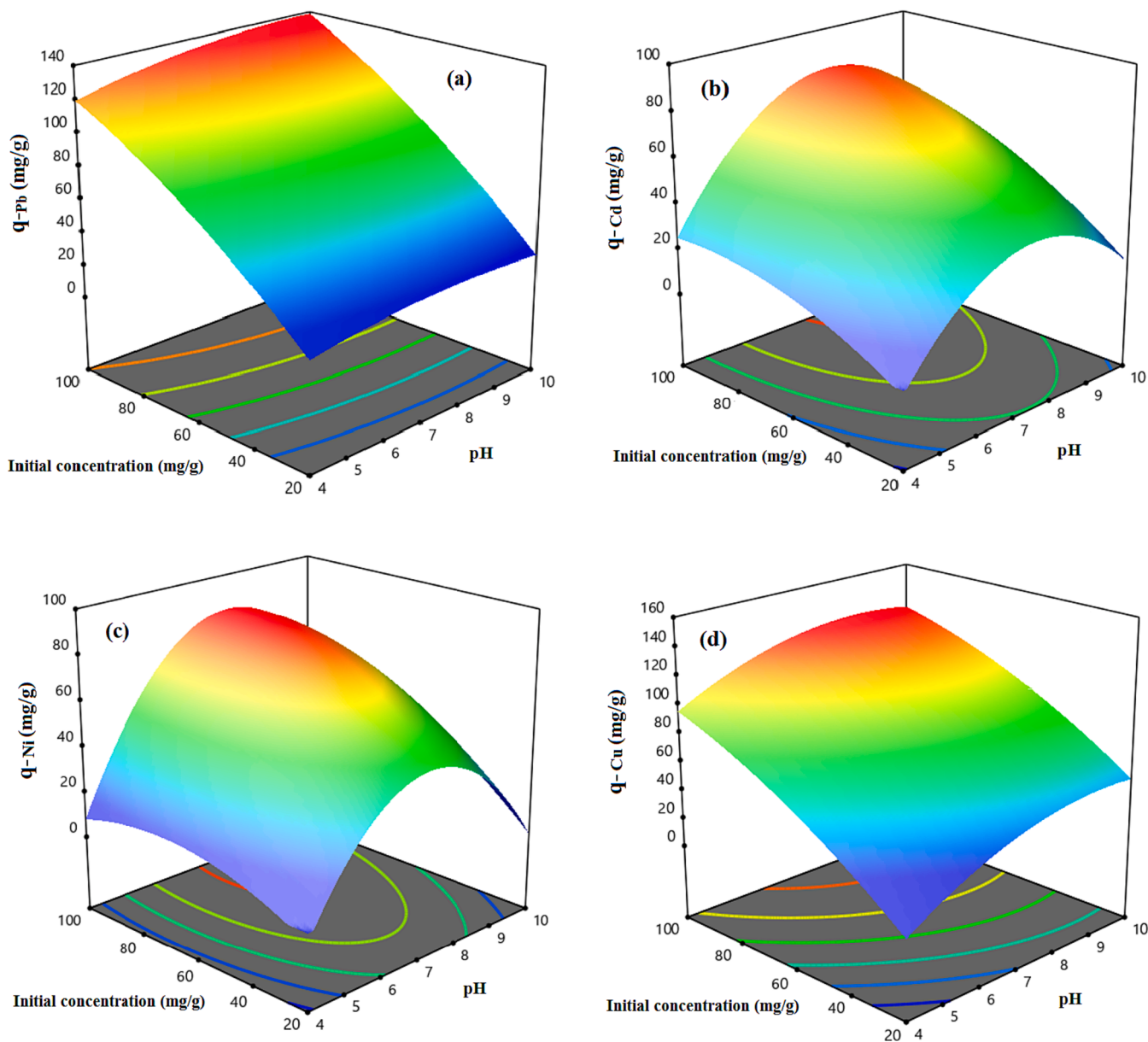


Fig. 10. 3D response surfaces representing the HCP adsorbent's uptake capacity dependency to the pH and initial concentration at pH of 7, for a) Lead, b) Cadmium, c) Nickel, d) Copper.

can separate the mesopores volume to multiple micropores (Li, 2017). The elemental composition of the polymeric samples were investigated by using EDS analysis and the findings of the analysis are depicted in Fig. 5. According to the EDS analysis results, the xylene based HCP adsorbent consist of 94.62 % carbon, 4.12 % oxygen, and 1.26 % chlorine element that can be related to the Lewis acid catalyst in the Friedel-Craft alkylation reaction, also the modified HCP sample contains 78.58 % carbon, 3.48 % manganese, 16.73 % oxygen, and 1.21 % chlorine. Increasing the oxygen content of the modified HCP adsorbent corresponds to the incorporation of carboxylic acid into the HCP sample structure. The XPS spectra of the unmodified/modified HCP samples in the range of 100 eV to 800 eV are illustrated in Fig. 6-a. based on this figure, the resulting peaks at 198.6 eV, 285.9 eV, and 533.1 eV are attributed to Cl 1s (1.09 %), C 1s (80.64 %), and O 1s (18.27 %), respectively. The ionic form of the chlorine element (Cl^-) may be left over from the Friedel-Crafts reaction (Sang et al., 2020). By considering the high-resolution spectrum of the C 1s element that is illustrated in Fig. 6-b, it can be derived that the mentioned peak dissociated to three

peaks correspond to C—C/C=C bonds (284.6 eV), C—OH bond (286.5 eV), and COOH bond (289.4 eV). Fig. 6-c demonstrates that the O 1s spectrum has two unique peaks that are related to the carboxylic acid's C=O bond (532.7 eV) and the C—OH bond (533.6 eV) (Manakhov, 2023; Zhang, 2013; Classen, 2007; Beamson and Briggs, 1992; Song, 2021).

3.2. RSM results

3.2.1. Analysis of variance (ANOVA)

Analysis of variance of the lead, cadmium, nickel, and copper ions adsorption capacity (q) in the multi component system are provided in terms of temperature, pH, and initial concentration of the metallic ions. The findings are reported in Table 3 and Table 4 for xylene based HCP and carboxylic acid modified HCP adsorbent, respectively. In ANOVA, P-value and F-value are two criteria that demonstrate the significance of the resulting model or model's terms. The P-value less than 0.05 and F-value more than 1 refer to model importance also the F-value greater

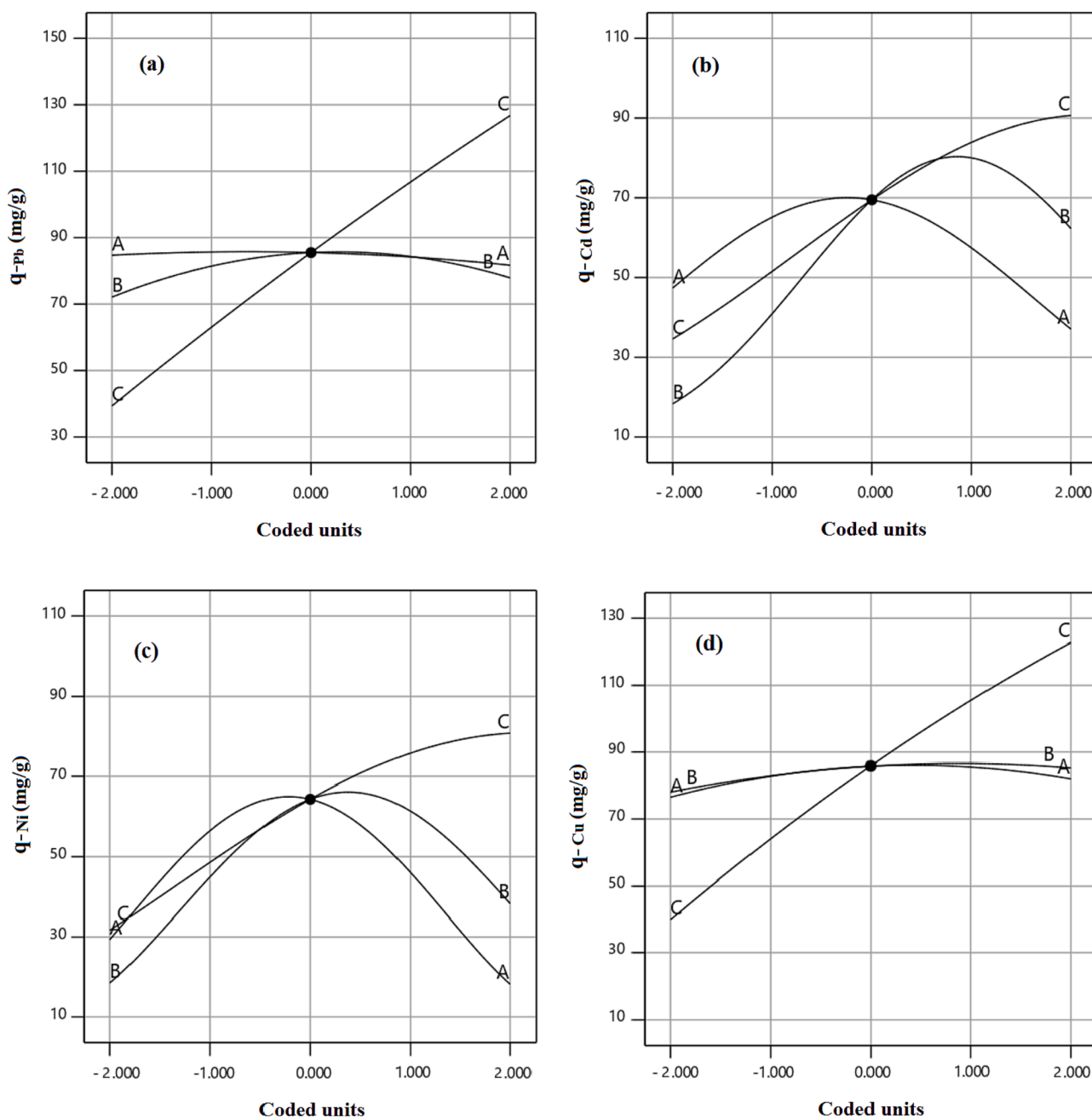


Fig. 11. Perturbation plots of the heavy metal uptake by carboxylic acid modified HCP a) Lead, b) Cadmium, c) Nickel, d) Copper.

than 0.1 and the F-value less than 1 indicate the model or model terms are not important. Based on Table 3 and Table 4 findings, the resulting models for prediction of the adsorption capacity of the lead (q_{Pb}), cadmium (q_{Cd}), nickel (q_{Ni}), and copper (q_{Cu}) using the xylene based HCP and carboxylic acid modified HCP adsorbents have P-value less than 0.0001 and F-value much more than 1, it means that the obtained models are significant. Adequate precision in a criteria of ANOVA which evaluate signal to noise ratio of the model, the adequate precision index higher than 4 proves that the resulting model has enough accuracy. The adequate precision values of the models for q_{Pb} , q_{Cd} , q_{Ni} , and q_{Cu} were obtained at 96.10, 27.34, 32.57, and 24.82 when the xylene based HCP was used as adsorbent and when the carboxylated HCP was applied as adsorbent, the adequate precision of the models were obtained 280.82, 24.11, 64.08, and 40.84 for q_{Pb} , q_{Cd} , q_{Ni} , and q_{Cu} , respectively. The models adequate precision values are much more than 4, it means that the obtained models are significant and they are applicable for process

design purposes in design space (Bashir et al., 2010). Correlation coefficients (R^2) value of the models are greater than 0.98, also the models adjusted R^2 values have good agreement with predicted R^2 values due to their little difference (difference is less than 0.2). By considering the R^2 values of the models, it can be concluded that the predicted data have good accordance with experimental data and the models have enough accuracy in design space.

3.2.2. Adsorption models

The semi-empirical quadratic models for prediction of the adsorption capacity of the metallic ions in terms of operational condition were obtained based on the RSM-CCD technique. The adsorption models for prediction of adsorption capacity of the lead, cadmium, nickel, and copper ions by utilizing xylene based HCP are presented in equations (7–10), respectively. In addition, the adsorption models for the uptake of mentioned metallic ions by carboxylic acid modified HCP adsorbent are

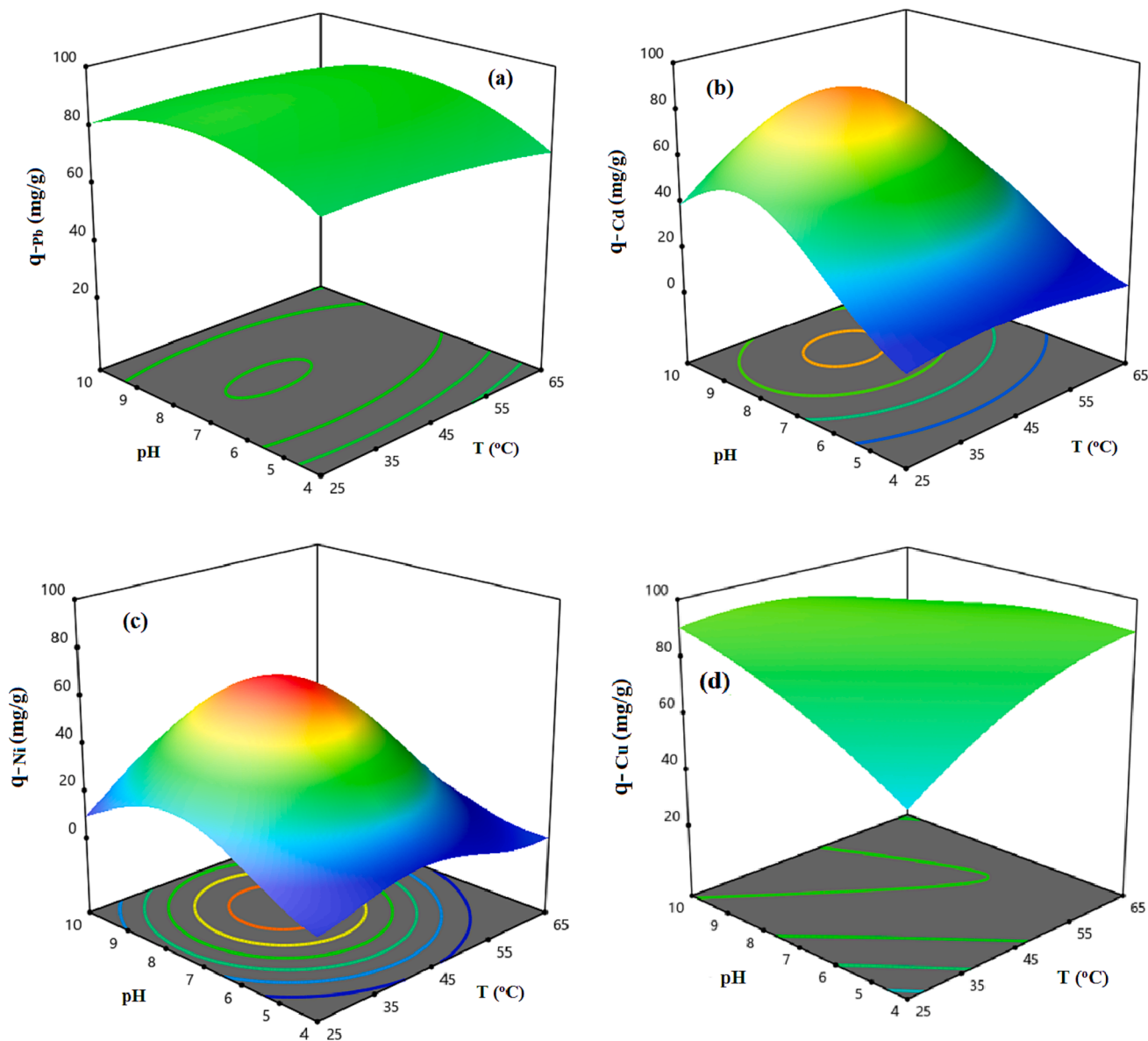


Fig. 12. 3D response surfaces representing the carboxylic acid modified HCP adsorbent's uptake capacity dependency to the pH and temperature at initial concentration of 60 mg/l for a) Lead, b) Cadmium, c) Nickel, d) Copper.

reported in equations (15–22), respectively. Furthermore, Fig. 7 (a-h) illustrate the contrast between the predicted heavy metal uptake capacities using the RSM-based model and the actual values. The figures indicate that by taking into account the adequate concentration of the predicted and the actual values adsorption capacity across the diagonal line, the superior accuracy of the presented semi-empirical models can be demonstrated.

$$q_{Pb} = -40.27727 + 0.652332*A + 6.49363*B + 1.48448*C + 0.039000*AB + 0.006656*AC + 0.025875*BC - 0.014517*A^2 - 0.545567*B^2 - 0.005298*C^2 \quad (15)$$

$$q_{Cd} = -524.06385 + 12.00843*A + 64.87823*B + 2.50028*C - 0.287125*AB - 0.031859*AC + 0.061104*BC - 0.099209*A^2 - 3.64901*B^2 - 0.007088*C^2 \quad (16)$$

$$q_{Ni} = -485.35051 + 10.28783*A + 73.30781*B + 1.39564*C - 0.23208*AB - 0.003153*AC + 0.113104*BC - 0.114150*A^2 - 5.37443*B^2 - 0.011220*C^2 \quad (17)$$

$$q_{Cu} = -23.74753 + 3.10602*A + 34.67724*B + 2.13802*C - 0.036875*AB - 0.008259*AC + 0.032813*BC - 0.035682*A^2 - 1.73748*B^2 - 0.008003*C^2 \quad (18)$$

$$q_{pb} = -68.33282 + 0.362097*A + 16.01616*B + 1.66074*C + 0.014750*AB - 0.000450*AC + 0.013000*BC - 0.005754*A^2 - 1.16871*B^2 - 0.002746*C^2 \quad (19)$$

$$(q_{Cd})^{0.15} = -1.09120 + 0.034829*A + 0.433140*B + 0.011813*C + 0.000291*AB - 0.000035*AC + 0.000423*BC - 0.000413*A^2 - 0.28186*B^2 - 0.000079*C^2 \quad (20)$$

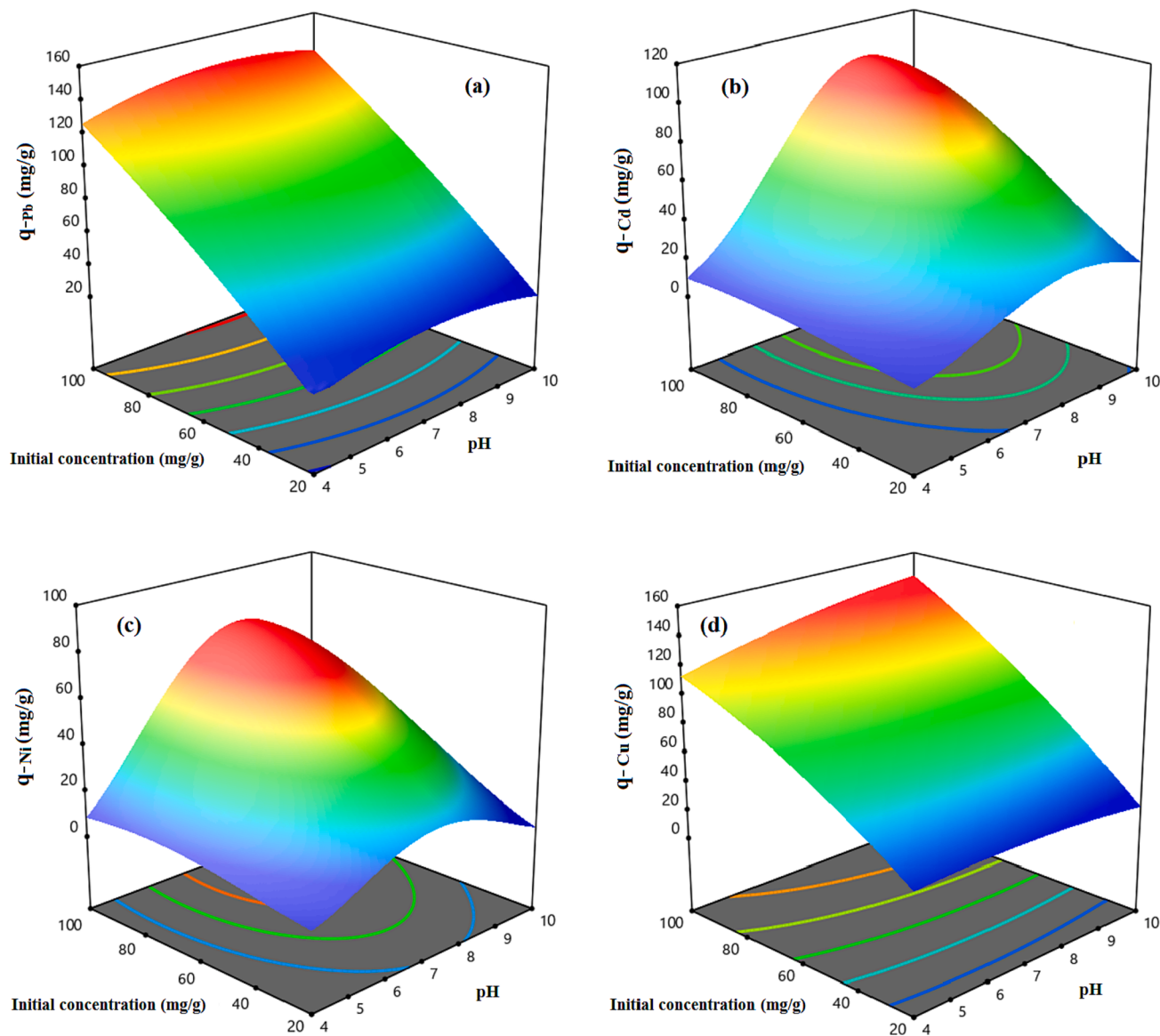


Fig. 13. 3D response surfaces representing the carboxylic acid modified HCP adsorbent’s uptake capacity dependency to the pH and initial concentration at pH of 7, for a) Lead, b) Cadmium, c) Nickel, d) Copper.

Table 5
Optimal condition respect to maximization of the lead uptake selectivity by xylene-based HCP and modified HCP sample.

Sorbent	Parameter and response	Target	Lower limit	Higher limit	Optimal condition		AARD%
					RSM	Experimental	
Xylene based HCP	Temperature (°C)	In range	25	65	31.8		
	pH	In range	4	10	5		
	Initial concentration (mg/l)	In range	20	100	82.5		
	Pb(II) uptake capacity (mg/g)	Maximize	29.805	133.29	105.37	103.74	1.57
	Cd(II) uptake capacity (mg/g)	Minimize	10.94	84.37	44.68	42.96	4
	Ni(II) uptake capacity (mg/g)	Minimize	8.714	84.02	32.07	34.14	6.06
	Cu(II) uptake capacity (mg/g)	Minimize	27.91	128.82	83.1	82.48	0.75
	Selectivity(Pb/Cd) = 2.41, Selectivity(Pb/Ni) = 3.03, Selectivity(Pb/Cu) = 1.25						
Carboxylic acid modified HCP	Temperature (°C)	In range	25	65	30		
	pH	In range	4	10	5.5		
	Initial concentration (mg/l)	In range	20	100	100		
	Pb(II) uptake capacity (mg/g)	Maximize	29.83	141.06	136.93	135.47	1.07
	Cd(II) uptake capacity (mg/g)	Minimize	11.57	93.52	31.07	32.96	5.73
	Ni(II) uptake capacity (mg/g)	Minimize	6.308	65.35	22.87	21.04	8.69
	Cu(II) uptake capacity (mg/g)	Minimize	29.95	135.24	104.61	102.43	2.12
	Selectivity(Pb/Cd) = 4.11, Selectivity(Pb/Ni) = 6.43, Selectivity(Pb/Cu) = 1.32						

Table 6
Characteristics of the steel industry waste water.

Parameters	Characteristics
pH	6.7
Total solids (mg/l)	15,800
BOD (mg/l)	<2.0
COD (mg/l)	<2.0
Cl ⁻ (mg/l)	381
SO ₄ ²⁺ (mg/l)	963
Ca ²⁺ (mg/l)	2846
Mg ²⁺ (mg/l)	328
HCO ₃ ⁻ (mg/l)	341
Mn ²⁺ (mg/l)	26.5
Cd ²⁺ (mg/l)	2.7
Fe ²⁺ (mg/l)	40.3
Zn ²⁺ (mg/l)	10.6
Ni ²⁺ (mg/l)	8.7
Cu ²⁺ (mg/l)	1.3

$$(q_{Ni})^{0.45} = -24.45907 + 0.605728*A + 3.76580*B + 0.084171*C + 0.002274*AB - 0.000190*AC + 0.006087*BC - 0.007139*A^2 - 0.275649*B^2 - 0.000714*C^2 \quad (21)$$

$$q_{Cu} = -82.40925 + 2.33099*A + 12.46638*B + 0.811348*C - 0.188542*AB + 0.012222*AC + 0.075146*BC - 0.016481*A^2 - 0.465378*B^2 - 0.005058*C^2 \quad (22)$$

3.2.3. Effect of operational factors on adsorption process

3.2.3.1. Adsorption by xylene based HCP. To peruse the impact of operational factors including temperature, pH, and initial concentration of the solution on the metallic ions uptake capacity of the xylene based HCP adsorbent, perturbation plots are provided and illustrated in Fig. 8. In these plots, the A, B, and C curves indicate the impact of variation of the temperature, pH, and initial concentration on adsorption capacity. By default, the reference point of the perturbation plot was considered at the center point of the design space with a coded value equal to 0, the actual value of the A, B, and C terms at the reference point are 45 °C, 7, and 60 mg/l, respectively. According to Fig. 8, heavy metal ions

adsorption by HCP adsorbent is strongly affected by increasing the initial concentration of metallic ions in the solution, but the effect of the other factors on uptake capacity is dependent on the adsorbed metal ion type. As can be seen in Fig. 8.a, the lead ion adsorption by HCP adsorbent is not sensitive to the temperature and pH alteration due to the A and B curves status which are near to the horizontally state. According to Fig. 8.b and Fig. 8.c, the cadmium and nickel uptake are deeply influenced by changing temperature and pH value, and the maximum adsorption capacity of these ions are obtained at a temperature of 45 °C and pH of 7. Based on Fig. 8.d, the copper adsorption capacity can increase by gaining pH value up to 9 at the reference point of temperature and initial concentration. To better understand of the mentioned factors effect on HCP adsorbent's uptake capacity and investigation of the factors interaction, three dimensional response surfaces are provided based on RSM model that are illustrated in Fig. 9 and Fig. 10. The Fig. 9 depicts the HCP adsorbent's uptake capacity dependency to temperature and pH at a constant initial concentration of 60 mg/l. Based on the figure, the maximum uptake capacity of lead ion can be obtained at about 87.5 mg/g at T = 50 °C and pH = 9, also for cadmium and nickel adsorption by HCP adsorbent, a similar condition is observed in which maximum adsorption capacity of these ions at T = 45 °C and pH = 7 are obtained 58.67 mg/g and 64.81 mg/g, respectively. According to Fig. 9. d, the highest adsorption capacity of copper ion at the initial concentration of 60 mg/g, can be reached at T = 45 °C and pH = 9. Based on the figures findings, the solution pH has a key role in the heavy metals adsorption capability of HCP adsorbent. In general, decreasing in solution's pH causes a reduction in the uptake capacity of the metallic ions, this happens due to gaining in hydronium ions (H₃O⁺) concentration which result in improving the repulsion force between hydronium ions and metallic ions, also increasing the pH of the solution (pH greater than 9) causes the formation of metal hydroxide and decreases the adsorption capacity of HCP adsorbent (Qin, 2019). Fig. 10 depicts effect of the pH and initial concentration of metallic ions on the HCP uptake capability at a constant temperature of 45 °C. According to Fig. 10, at a constant pH value, increasing the initial concentration of the ions causes improving the uptake capacity of the solid sorbent, it can be attributed to the improving mass transfer driving force and diminished mass transfer resistance of the metallic ions diffusion into the HCP adsorbent's cavities (Gonte and Balasubramanian, 2016). Based on the findings, the uptake capacity of the metallic ions by xylene based HCP sample at a similar condition are in descending order Pb²⁺ > Cu²⁺ > Ni²⁺ > Cd²⁺.

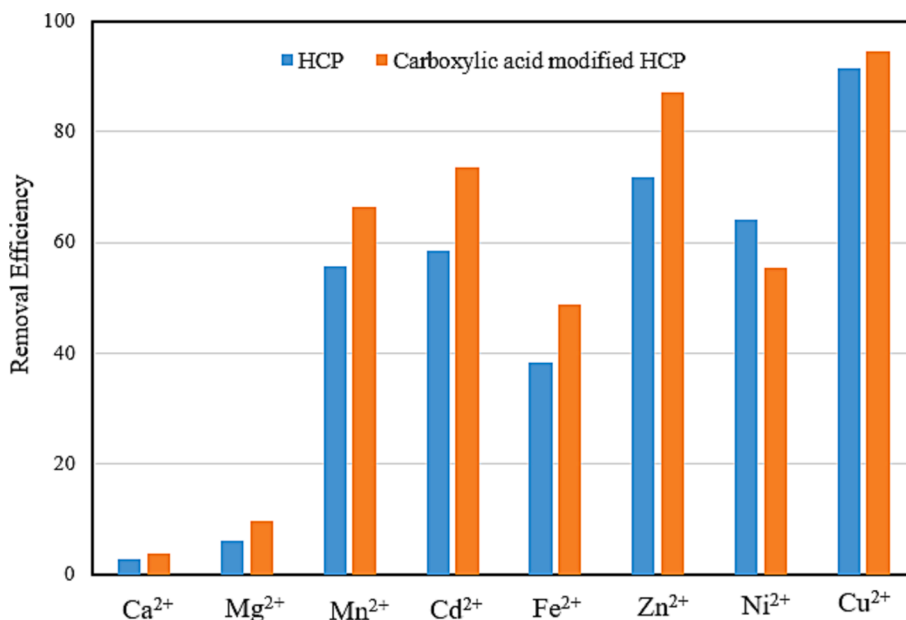


Fig. 14. Removal efficiency of the metallic ions uptake from steel industry waste water.

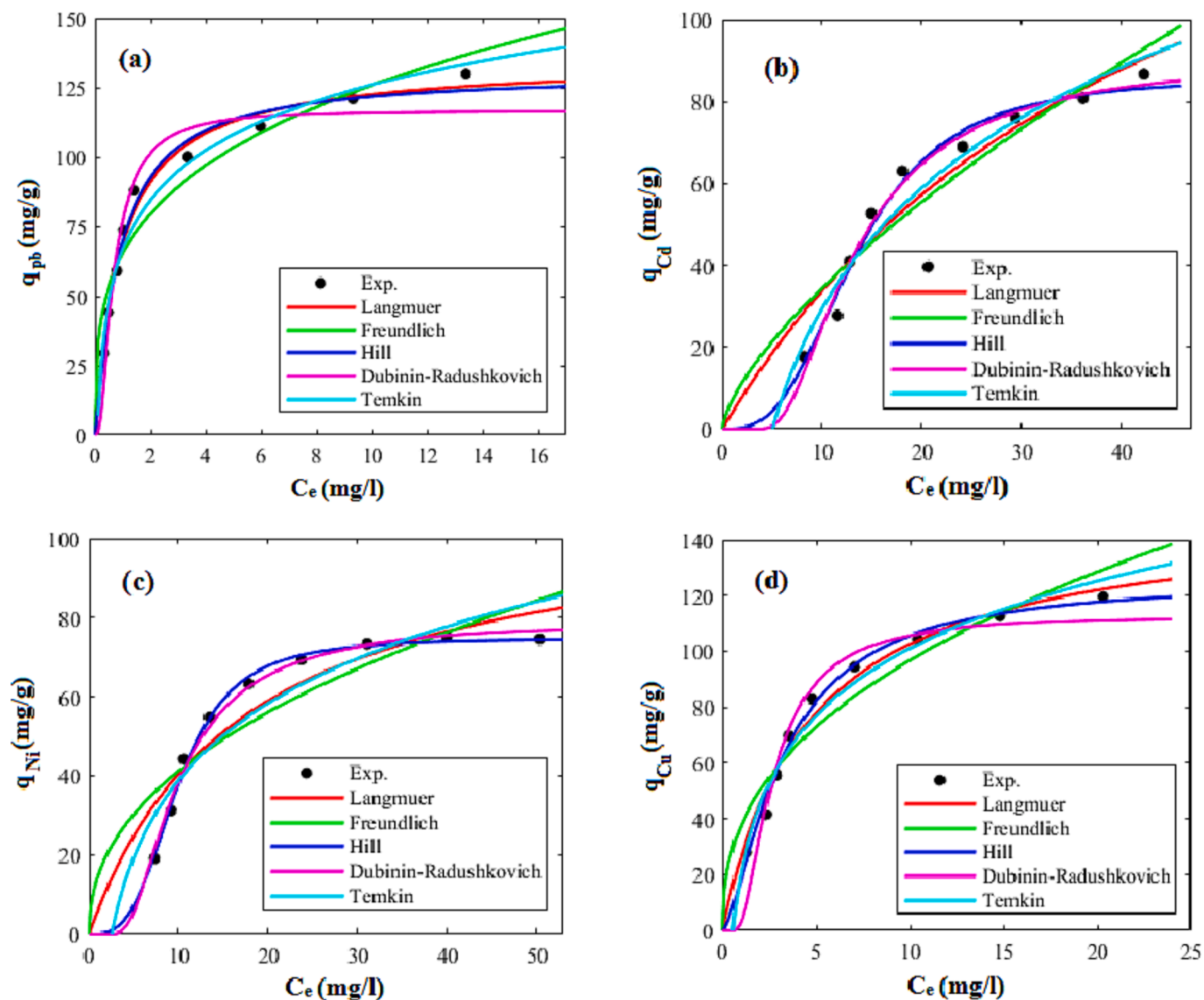


Fig. 15. Comparison of isotherm models and experimental values of adsorption capacity of xylene based HCP at 35 °C and pH = 7 for uptake of (a) lead (b) cadmium, (c) nickel, (d) copper.

3.2.3.2. Adsorption by carboxylic acid modified HCP. Similar to xylene based HCP adsorbent, the heavy metal uptake capacity of the carboxylic acid functionalized HCP adsorbent is studied in this section. To investigate the effect of temperature, pH, and solution initial concentration on the uptake capacity of the functionalized HCP, perturbation plots are prepared and illustrated in Fig. 11. According to the Fig. 11.a, slightly gaining in lead ion uptake capacity by carboxylic acid modified HCP sample is observed. Based on Fig. 11.b and Fig. 11.c, the adsorption capacity of the cadmium and nickel ions are deeply affected by changing the temperature and pH value of the solution. Compare to xylene based HCP sample, the carboxylic acid modified HCP sample shows more adsorption capacity for cadmium and nickel ions at pH value more than 7, it can be related to the presence of the hydroxide ions (OH^-) in the solution which causes deprotonating the carboxylic acid groups and making this group as an active site for chelate formation or exchanging heavy metal ions (Ehgartner, 2021). According to these figures, increasing the pH value more than 8.5 will be decreased the adsorption capacity of the cadmium and nickel ions, it can be attributed to the formation of the metal hydroxide in the solution.

Aim to show the modified HCP sample uptake capability dependency to the mentioned parameters and investigation of the factors interaction,

the three dimensional response surfaces are illustrated in Fig. 12 and Fig. 13. The Fig. 12 indicates the effect of the temperature and pH on the uptake capacity at a constant initial concentration equal to 60 mg/l. According to Fig. 12.a, the highest uptake capacity of the lead ion ($q = 88.6$ mg/g) can be obtained at $T = 35$ °C and $pH = 7.5$, also similar is observed for copper ion adsorption capacity based on Fig. 12.d. Based on this figure, the maximum value of adsorption capacity of the copper ion ($q = 87.9$ mg/g) at the initial concentration of 60 mg/l can be obtained at $T = 50$ °C and $pH = 8.5$. Fig. 12.b and Fig. 12.c show that the highest adsorption capacity of the cadmium and nickel ions can be obtained at $T = 45$ °C and $pH = 8.5$ and $T = 45$ °C and $pH = 8$, respectively. Fig. 13 depicts the heavy metal uptake capacity dependency to the metal ions initial concentration and the solution's pH value at a constant temperature of 45 °C. According to Fig. 13, by increasing the initial concentration of the solution, the uptake capacity of the metallic ions are increased dramatically due to improving the mass transfer driving force. Based on Fig. 13 results, it can be concluded that increasing the initial concentration of the solution to more than 80 mg/l slightly improves the adsorption capacity of the cadmium and the nickel ions, however, the lead and the copper ions uptake capacities will be increased sharply even at higher initial concentration, it can be related to the adsorbent

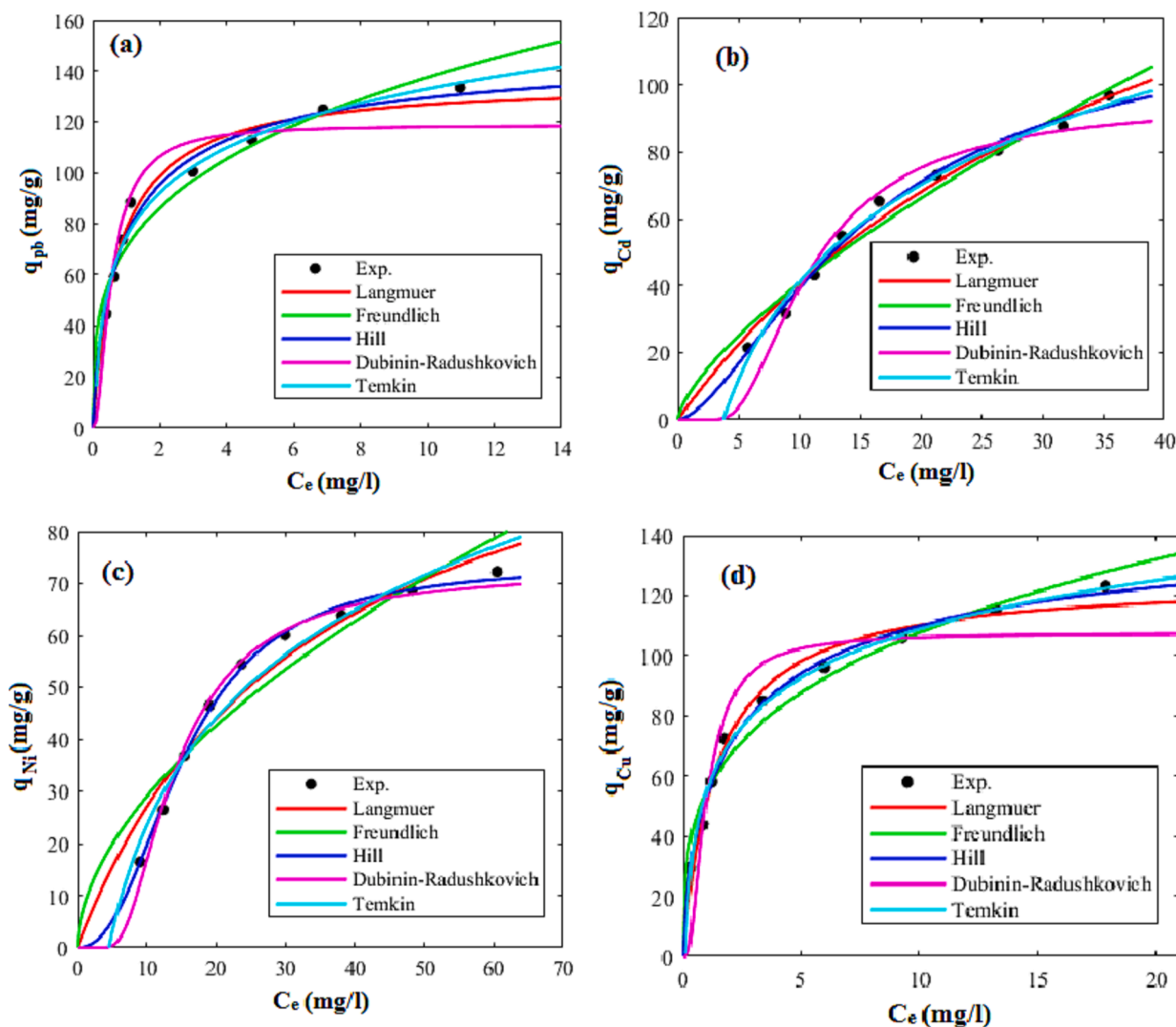


Fig. 16. Comparison of isotherm models and experimental values of adsorption capacity of carboxylic acid modified HCP at 35 °C and pH = 7 for uptake of (a) lead (b) cadmium, (c) nickel, (d) copper.

saturation from the cadmium and the nickel ions at the concentration more than 80 mg/l (Vakili, 2019). Based on the results, the heavy metal ions uptake capacity of the carboxylic acid functionalized HCP sample at the reference point are in descending order $Pb^{2+} > Cu^{2+} > Cd^{2+} > Ni^{2+}$.

3.2.4. Process optimization

In the context of adsorption and separation of the lead ion from multi component solution using both types of the adsorbents, high selectivity towards lead metal is crucial for practical applications. It should be noted that achieving superior selectivity of the lead over other metals in the adsorption process is contingent upon maximizing the uptake capacity of the lead and minimizing the adsorption capacity of the other metals. Therefore, operational factors namely temperature, pH, and initial concentration should be optimized to achieve the highest efficiency. In this study, the process optimization was applied using Design Expert software optimization module. Specifically, the desired target for lead uptake capacity was set to “maximize”, while the uptake capacities of other cations such as cadmium, nickel, and copper were set to “minimize”, also the mentioned operating factors were selected to be “in range” for optimal results. To check the validity of the resulting metallic ions adsorption capacities in the optimal condition, two adsorption experiments were conducted under the determined optimal operational conditions using both types of adsorbents, also Absolute Average

Relative Deviation (AARD%) were calculated aim to assess error between experimental and RSM based results. The results of the process optimization for both polymeric samples are summarized in Table 5. Based on Table 5 findings, it can be concluded the adsorption capacities obtained by the xylene based HCP at the optimum condition namely temperature of 31.8 °C, pH of 5.0, and initial concentration of 82.50 mg/l were in satisfactory agreement with the RSM result, with an average error of 3.09 %. Similarly, the uptake capacities obtained by the modified HCP sample at the optimum condition such as temperature of 30.0 °C, pH of 5.5, and initial concentration of 100 mg/l exhibited a good agreement, with an average error of 4.40 %. Based on the Table 5 results, chemically modification of the xylene based HCP sample improved the selectivity of the lead ion uptake over other metal ions. Especially, the selectivity of the lead over cadmium increased from 2.41 to 4.11, and the selectivity of the lead uptake over nickel gained from 3.03 to 6.43, also slightly increasing in the lead adsorption selectivity from 1.25 to 1.32 was observed due to incorporation of the carboxylic acid group to the HCP sample skeleton.

3.3. Heavy metal adsorption from steel industry waste water

To investigate the potential of the HCP adsorbents for the removal of the heavy metal ions from steel industry waste water, metallic ions

Table 7

Isotherm models parameters of lead, cadmium, nickel and copper ions uptake by HCP and carboxylic acid modified.

Isotherm model	Parameters	Xylene based HCP				Carboxylic acid modified HCP			
		T = 35 °C and pH = 7				T = 35 °C and pH = 7			
		Cu ²⁺	Ni ²⁺	Cd ²⁺	Pb ²⁺	Cu ²⁺	Ni ²⁺	Cd ²⁺	Pb ²⁺
Langmuir	$q_m K_L R^2$	150.17	109.12	188.63	134.20	125.84	93.88	209.98	136.29
		0.215	0.0587	0.0217	1.0527	0.7047	0.0432	0.0240	1.3211
		0.979	0.927	0.938	0.971	0.970	0.917	0.960	0.979
Freundlich	$K_F n_f R^2$	37.67	14.749	7.039	65.177	54.52	10.538	8.128	70.57
		2.442	2.244	1.451	3.5	3.386	2.162	1.428	3.451
		0.935	0.887	0.902	0.936	0.943	0.871	0.963	0.72
Hill	$q_m K_h n_h R^2$	125.76	74.67	86.085	130.64	150.78	63.44	119.2	151.93
		5.82	1809.9	2077.1	0.87	1.854	2876.2	78.36	1.003
		1.483	3.269	2.935	1.108	0.687	3.060	1.587	0.785
D-R	$q_m \lambda E R^2$	0.996	0.997	0.991	0.992	0.996	0.994	0.995	0.992
		112.95	79.14	90.85	116.87	107.59	72.65	94.79	118.70
		1.114	12.15	21.71	0.133	0.227	24.72	14.80	0.10
Temkin	$\frac{RT}{b_T} A_T R^2$	0.670	0.203	0.152	1.939	1.484	0.142	0.184	2.233
		0.977	0.995	0.990	0.975	0.942	0.995	0.975	0.958
		34.88	28.13	42.54	25.84	23.41	29.93	41.95	25.35
		1.811	0.397	0.200	13.07	10.44	0.218	0.267	19.03
		0.985	0.933	0.976	0.984	0.995	0.981	0.994	0.991

Table 8

Kinetic models parameters of the heavy metal adsorption by HCP and carboxylic acid modified.

Sample	Kinetic model	Parameter	T = 25 °C and pH = 7				T = 35 °C and pH = 7			
			Pb ²⁺	Cd ²⁺	Ni ²⁺	Cu ²⁺	Pb ²⁺	Cd ²⁺	Ni ²⁺	Cu ²⁺
Xylene based HCP	Pseudo-first-order	q_e	116.66	77.54	43.16	99.63	122.22	72.9	57.75	106.14
		K_1	0.2593	0.2612	0.2593	0.2721	0.2808	0.2621	0.2593	0.2613
		R^2	0.933	0.948	0.965	0.941	0.938	0.953	0.967	0.948
	Pseudo-second-order	q_e	127.76	84.88	47.27	108.79	133.2	79.8	63.24	116.19
		$K_2 \times 10^3$	2.892	4.391	7.817	3.605	3.063	4.689	5.843	3.208
		R^2	0.999	0.998	0.999	0.997	0.999	0.999	0.998	0.999
	q_{exp}	123.54	82.795	46.51	106.55	129.42	78.875	62.885	113.93	
Carboxylic acid modified HCP	Pseudo-first-order	q_e	133.92	51.95	27.19	104.50	135.09	70.59	55.67	117.77
		K_1	0.2729	0.2612	0.2593	0.2538	0.2728	0.2572	0.2518	0.2451
		R^2	0.924	0.950	0.952	0.933	0.931	0.948	0.959	0.946
	Pseudo-second-order	q_e	146.33	56.87	29.78	114.52	147.61	77.33	61.05	129.36
		$K_2 \times 10^3$	2.681	6.554	12.40	3.151	2.656	4.735	5.841	2.667
		R^2	0.998	0.999	0.997	0.998	0.999	0.997	0.999	0.998
	q_{exp}	143.45	55.80	29.67	111.77	144.68	76.43	60.70	127.41	

uptake experiments were conducted at the optimum pH and temperature condition by utilizing the xylene based HCP and the carboxylic acid modified HCP samples. The waste water's characteristics are summarized in the Table 6. Based on the table, the pH value of the waste water is higher than optimum value, so it was adjusted to the optimum pH with the help of the HCl solution (0.05 M), followed by performing adsorption test. The results of measuring the removal efficiency of the metallic ions uptake are illustrated in Fig. 14. based on this figure, the carboxylic acid modified HCP sample exhibited more affinity to adsorb metallic ions than HCP sample except in the case of nickel adsorption, which is the opposite result.

3.4. Adsorption equilibrium study and isotherm modeling

To obtain the isotherm models' parameters, the models were fitted on the equilibrium adsorption data that obtained at the temperature of 35 °C, pH of 7, and initial concentration between 20 and 100 mg/l. The models' fitted curves were graphically illustrated in Fig. 15 and Fig. 16 for the xylene based HCP and the carboxylic acid modified HCP sample, respectively. Furthermore, the parameters of the models and their

correlation coefficients (R^2) were reported in Table 7. Based on the results presented in Table 7, the Freundlich model's K_F constant, which reflects the interaction strength between the adsorbed particles and the solid sorbent, indicates improving the lead, cadmium, and copper ions tendency to be adsorbed by the carboxylic acid modified adsorbent, but a relative decrease for nickel ion uptake by the modified HCP can be observed. The range of the Freundlich constant n_f , between 1 and 10, indicates that both adsorbents are suitable for the adsorption of metallic ions (Soltani et al., 2015). Furthermore, the dominant physical adsorption of the metallic ions by both adsorbents is shown by the E value being less than 8 kJ/mol, as determined by the Dubinin-Radushkevich model. According to the Hill isotherm model's q_m values which shows the best fitting ability for correlating experimental data, the adsorption tendency of metallic ions follows the sequence of lead > copper > cadmium > nickel. The sequence of the metal ions adsorption and lead selective removal can be explained as follows: (I) the larger electronegativity difference between lead (2.33) and nickel (1.91), cadmium (1.69), and copper (1.90), makes the lead as the best candidate to be attracted by adsorbent surface (Taha et al., 2016). (II) The ionic radius of the metallic ions are in a descending order lead (1.33 Å) > cadmium

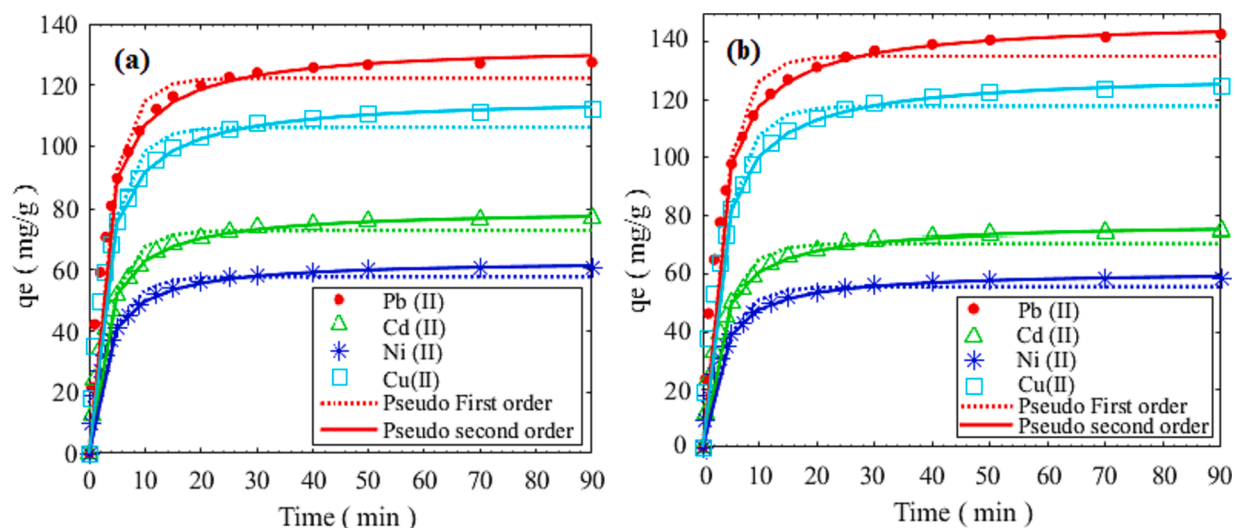


Fig. 17. Comparison of kinetic models and experimental values of adsorption capacity of lead, cadmium, nickel, copper at 35 °C and pH = 7 by (a) xylene based HCP, (b) carboxylic acid modified HCP.

Table 9

Results of the similar works on heavy metal adsorption from multi component systems.

Adsorbent	Operational condition			Adsorbate	Adsorption capacity (mg/g)	Ref.
	T (K)	pH	C ₀ (mg/l)			
SHCP-1	293	7	1230, 817	Cs ⁺ , Sr ²⁺	42.05, 63.3	(James, 2019)
UiO-66-NDC/GO	298	6	250	Pb ²⁺	254.45	(Singh, 2023)
Carboxylated MWCNT	298	8	50	Cd ²⁺	59.7	(Alimohammady et al., 2018)
Pyrazole MWCNT	298	7.95	50	Cd ²⁺	93.7	(Alimohammady et al., 2018)
MWCNT-COOH	298	7	50	Pb ²⁺	16.63	(Tahermansouri and Beheshti, 2013)
COOH@COF	298	6	10	Hg ²⁺ , Pb ²⁺	99.1, 123.8	(Lu, 2019)
MF-NTA	308	6	100	Cu ²⁺	29.7	(Baraka et al., 2007)
HTC-HCP	298	7	100	Cd ²⁺ , Pb ²⁺ , Ni ²⁺	60, 180, 20	(Yang, 2021)
SAM-HCPs	323	5.48	80	Cu ²⁺	57.68	(Li, 2011)
APTZ-PS	308	5, 6, 2	95, 310, 601	Cu ²⁺ , Pb ²⁺ , Hg ²⁺	59.0, 271.4, 220.6	(Zhang et al., 2014)
CSAP	303	5	100	Cu ²⁺ , Cd ²⁺ , Ni ²⁺	124, 84, 67	(Monier et al., 2012)
Kryptofix-22	298	7	20	Cd ²⁺ , Cr ³⁺ , Ni ²⁺	3.18, 3.72, 2.35	(Yilmaz, 2007)
SMA	298	6.7	200	Cu ²⁺ , Zn ²⁺ , Ni ²⁺	14.45, 15.13, 11.86	(Gonte and Balasubramanian, 2016)
cross-linked carboxymethyl corn starch	298	6	200	Cu ²⁺ , Pb ²⁺ , Cd ²⁺	127, 202.3, 193.3	(Kim and Lim, 1999)
cross-linked polyzwitterionic acid (CPZA)	298	6, 4	100	Cu ²⁺ , Pb ²⁺	1080, 1488	(Al Hamouz and Ali, 2012)
Chitosan/rectorie (CTS/REC) nano-hybrid	313	6	200	Cu ²⁺ , Cd ²⁺ , Ni ²⁺	20.49, 16.53, 13.32	(Zeng, 2015)
Xylene based HCP	308	7	100	Pb ²⁺ , Cd ²⁺	127.92, 89.11	This work
Carboxylic acid modified HCP	308	7	100	Ni ²⁺ , Cu ²⁺	73.51, 117.53	
				Pb ²⁺ , Cd ²⁺	135.54, 96.86	
				Ni ²⁺ , Cu ²⁺	62.23, 124.19	

(1.09 Å) > copper (0.87 Å) > nickel (0.83 Å). Metal with a larger ionic radius show more polarizability and more tendency to be adsorbed by heterogeneous surface (Bayo, 2012). (III) The hydrated radius of the lead, nickel, copper, and cadmium ions are 4.01 Å, 4.04 Å, 4.19 Å, and 4.26 Å, respectively. Metals with lower hydrated radii reveal more affinity to be adsorbed due to their easier diffusion into adsorbent pores. (IV) The enthalpy of hydration of the mentioned cations follows the sequence of lead (−1481 kJ/mol) < cadmium (−1807 kJ/mol) < copper (−2100 kJ/mol) < nickel (−2105 kJ/mol). Metal with higher enthalpy of hydration tend to be as hydrated and show lower affinity to be adsorbed, therefore the lead ion with the lowest enthalpy of hydration among other metallic ions preferentially adsorbed by solid sorbent (Panayotova and Velikov, 2003).

As a result, the above mentioned reasons are not able to determine individually the adsorption selectivity in a multi component system, so the simultaneously effect of the aforementioned explanations causes the heavy metal uptake sequence of Pb(II) > Cu(II) > Cd(II) > Ni(II). Similar result about adsorption sequence in a multi component system was reported by Bayo.J (Bayo, 2012).

3.5. Adsorption process kinetics

By fitting the kinetic models on the experimental heavy metal adsorption data, collected at the initial concentration of 100 mg/l, pH of 7, and different temperatures such as 25 °C and 35 °C, the models' parameters were obtained that are reported in Table 8. According to the Table 8, it is evident that the R² values more than 0.99 derived from the pseudo-second-order model were higher than those of the pseudo-first-order adsorption model. Furthermore, the estimated q_e values derived from the pseudo second-order model showed a strong correlation with the actual values (q_{exp}), indicating the reliability of the model for the adsorption system being studied. According to the proper fit of both kinetic models, it can be concluded that the adsorption process utilizing both HCP samples were occurred through chemical and physical adsorption mechanism simultaneously (Yang et al., 2018). The values of k₂ (Table 7) also suggested that the adsorption rates followed the sequence of Ni²⁺ > Cd²⁺ > Cu²⁺ > Pb²⁺. The fitted adsorption data and the predicted values based on the kinetic models are illustrated in Fig. 17-a, and Fig. 17-b for the HCP sample, and the carboxylic acid modified HCP sample, respectively.

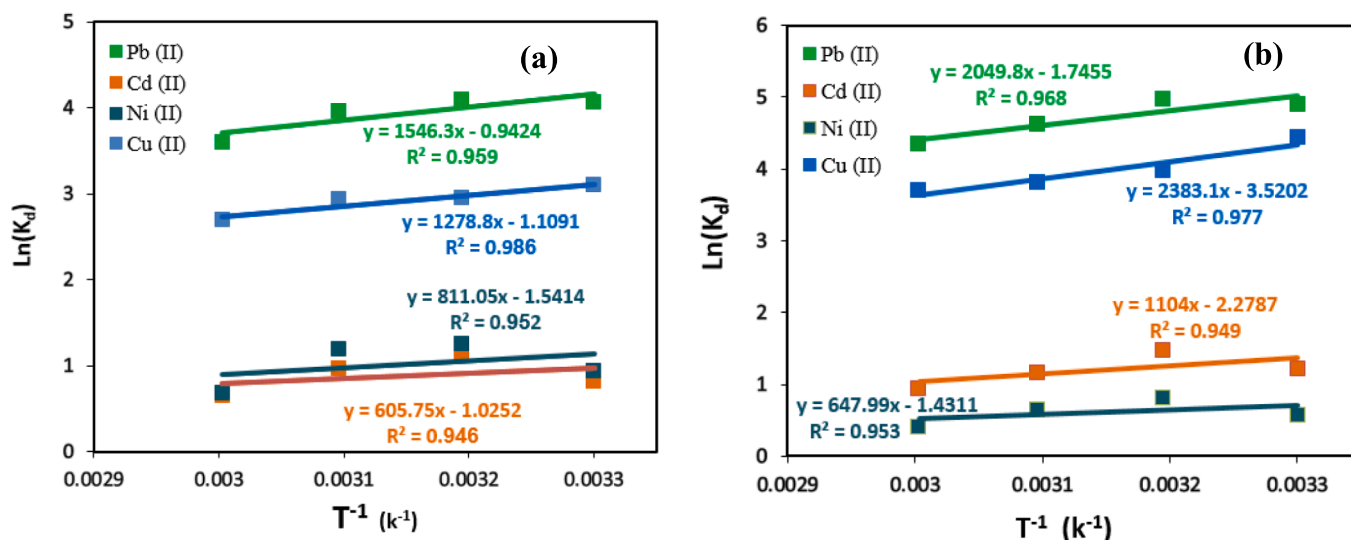


Fig. 18. Van't Hoff's plots for adsorption of lead, cadmium, nickel and copper ions by (a) HCP adsorbent (b) carboxylic acid modified HCP.

Table 10
Thermodynamic parameters of the heavy metal adsorption process.

Sample	Adsorbate	ΔH^0 (kJ/mol)	ΔS^0 (kJ/mol K)	ΔG^0 (kJ/mol)			
				303 K	313 K	323 K	333 K
Xylene based HCP	Pb ²⁺	-12.875	-0.008	-10.481	-10.403	-10.325	-10.246
	Cu ²⁺	-10.633	-0.009	-7.837	-7.745	-7.653	-7.560
	Ni ²⁺	-6.743	-0.0128	-2.858	-2.730	-2.601	-2.473
	Cd ²⁺	-5.036	-0.0085	-2.452	-2.367	-2.2819	-2.1967
Carboxylic acid modified HCP	Pb ²⁺	-17.034	-0.015	-12.634	-12.489	-12.344	-12.1989
	Cu ²⁺	-19.814	-0.029	-10.941	-10.649	-10.356	-10.0634
	Ni ²⁺	-5.3876	-0.01189	-1.7805	-1.661	-1.5425	-1.4235
	Cd ²⁺	-9.179	-0.0189	-3.435	-3.246	-3.056	-2.867

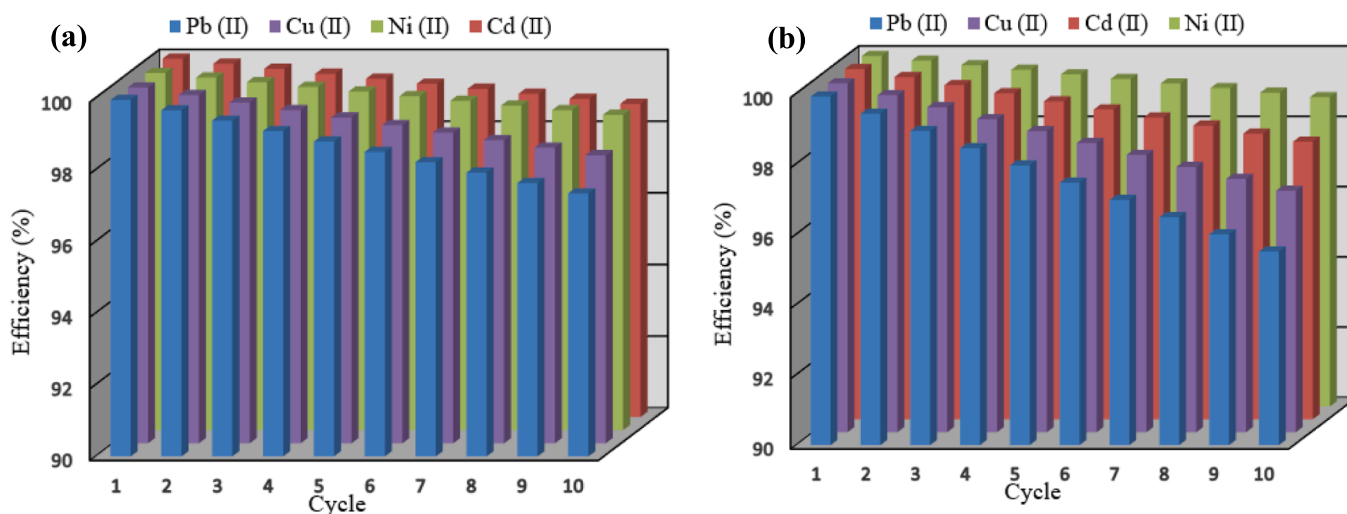


Fig. 19. Regeneration efficiency of (a) xylene based HCP, and (b) carboxylic acid modified HCP sample.

3.6. Comparison of the samples efficiency with similar studies

In this section, a comparison between the present work and similar studies on the heavy metal adsorption from multi component systems using porous polymeric adsorbents, was done. The results of the literature review are summarized in Table 9. As presented in the Table 7, the

xylene based HCP and the modified HCP sample show high overall uptake capacities of $q = 408.04$ mg/g and $q = 417.04$ mg/g, respectively. By comparing the results of the present study with other works in a similar operating condition, it can be concluded that both types of HCP adsorbents show high performance in simultaneously heavy metal adsorption in a multi component system.

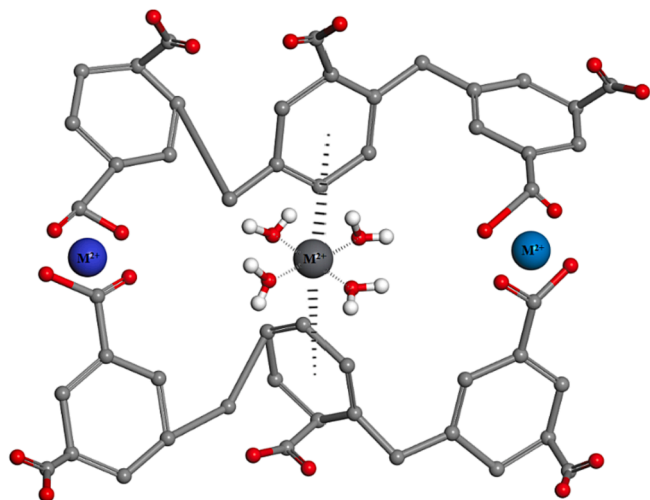


Fig. 20. Cation- π interaction and complexation mechanisms of the divalent heavy metal adsorption.

3.7. Thermodynamic modelling

In engineering processes, thermodynamic concepts such as entropy and Gibbs free energy are employed to assess the spontaneity of a process. Additionally, thermodynamic parameters can provide insight into the adsorption process's nature, particularly whether it involves an endothermic or exothermic. In the present research, the thermodynamic analysis of the heavy metal adsorption process was performed by computing the thermodynamic parameters, such as Gibbs free energy (ΔG°), entropy (ΔS°), and enthalpy (ΔH°) at a pH value of 7, an initial concentration of 60 mg/l, and the temperature between 30 °C and 60 °C, using equations (23–25).

$$\ln(K_d) = (\Delta S^\circ / R) - (\Delta H^\circ / RT) \quad (23)$$

$$K_d = \frac{(C_0 - C_e)}{C_e} (V/m) \quad (24)$$

$$\Delta G^\circ = \Delta H^\circ - T\Delta S^\circ \quad (25)$$

In the above equations, the terms V, m, and T are the solution's volume, the sample's weight, and the temperature of the adsorption process, respectively. The terms of K_d and R, refer to the distribution factor and global gas constant, respectively (Dizaj Khalili and Ghaemi, 2021). Van't Hoff diagrams which are illustrated in Fig. 18, were obtained by plotting the distribution factor values ($\ln(K_d)$) versus the inverse of temperature ($1/T$). According to Fig. 18, the slope of Van't Hoff's diagram represents the value of enthalpy, while the y-intercept of the diagram represents the value of entropy. The values of Gibbs free energy for an adsorption process can be calculated using equation (25). The thermodynamic parameters obtained from the adsorption of metallic ions by both types of the HCP samples are summarized in Table 10. Generally, the enthalpy range of the physical adsorption process is considered to be lower than 20 kJ/mol. On the other hand, chemical adsorption causes the production of enthalpy greater than 40 kJ/mol due to chemical bonding. Negative values of ΔG° indicate a process occurred spontaneously and is thermodynamically favorable. Additionally, more negative values of ΔG° indicate a greater driving force for the adsorption process, resulting in a higher adsorption capacity (Ghaemi et al., 2022). According to the Table 10 results, the metallic ions uptake by both HCP adsorbents took place physically ($\Delta H^\circ < 20$ kJ/mol), and the adsorption process is exothermic due to negative sign of the enthalpy values. Also, by considering the negative ΔG° values of the adsorption process, it can be concluded that the metallic ions adsorption by both samples were occurred spontaneously. Also, more negative values of the Gibbs free

energy for adsorption process by carboxylic acid modified HCP adsorbent, refer to more tendency of the adsorbate particles to be adsorbed and more favorability of the adsorption process.

3.8. Regeneration efficiency of adsorbents

From an economic perspective, the reusability of the adsorbent is a critical factor for industrial applications. To assess the recyclability of the adsorbents, ten cycles of adsorption were performed at a temperature of 45 °C and a pH value of 7 using both types of adsorbents. To regenerate the spent samples, the adsorbents were subsequently mixed with 0.05 M hydrochloric acid (HCl) and stirred for 2 h. The results of the recycling efficiency are presented in Fig. 19. According to this figure, the adsorption potential of carboxyl group-modified HCP for adsorbing lead, cadmium, nickel, and copper decreased by 4.5 %, 2.1 %, 1.2 %, and 3.13 %, respectively. Additionally, the adsorption potential of xylene-based HCP for adsorbing lead, cadmium, nickel, and copper reduced by 2.66 %, 1.26 %, 1.2 %, and 1.96 %, respectively, after ten cycles. Based on the results, both types of adsorbents could be considered as high-value adsorbents for industrial applications due to the slight decrease in their efficiency.

3.9. Adsorption mechanism

The heavy metal ions adsorption by the HCP sample is affected by several factors, such as the chemical properties of the sorbent and the physicochemical characteristics of the metal ions. The interaction between the sorbent and the metal ions occurs through various mechanisms, such as coordination, ion exchange, and electrostatic attraction (Wu, 2013; Zare-Dorabei et al., 2016). Specifically, the HCP network exhibits a chelating interaction between its carboxyl groups and the heavy metal ions, leading to forming the stable complexes. Additionally, the benzene ring in the adsorbent structure participates in a cation- π interaction with the metal ions, enhancing the adsorption efficiency. Moreover, the HCP network's porous structure, which includes micro-, meso-, and macropores, provides a large surface area for the uptake of metallic ions. The HCPs are primarily composed of microporous material due to the presence of benzene co-monomers. This allows the multiple benzene rings of HCPs to generate strong cation- π interactions with metal ions. The heavy metal adsorption mechanisms including cation- π interaction and complexation are graphically illustrated in Fig. 20.

4. Conclusion

In this work, experimental investigation of the heavy metal adsorption process were conducted in a multi component system including lead, cadmium, nickel, and copper ions. Aim to evaluate the HCP material adsorption capability and the effect of chemical modification of the HCP adsorbent on the lead uptake selectivity over the other metals, the xylene based HCP and the carboxylic acid functionalized HCP samples were utilized as solid sorbent. Based on the results, FT-IR analysis proves the successfully incorporation of the carboxyl group to the HCP sample skeleton, also BET analysis refer to the decreasing of the specific surface area of the HCP sample after modification, from 237.73 m²/g to 153.43 73 m²/g. The RSM based optimization was conducted with respect to maximization of the lead uptake selectivity, and the optimal condition namely temperature of 31.8 °C, pH of 5.0, initial concentration of 82.50 mg/l, and temperature of 30.0 °C, pH of 5.5, initial concentration of 100 mg/l were obtained for the HCP sample and the modified HCP sample, respectively. The results of the selectivity investigation at the optimal condition showed that the chemically modification of the HCP sample increased the Pb/Cd selectivity from 2.41 to 4.11, the Pb/Ni selectivity from 3.03 to 6.43, and Pb/Cu selectivity from 1.25 to 1.32. According to thermodynamically study of the process, metallic ions adsorption by both types of the adsorbents were spontaneously ($\Delta G^\circ < 0$), and exothermic ($\Delta H^\circ < 0$), also enthalpy

values less than 20 kJ/mol prove the physically adsorption of the metallic ions. In conclusion, the resulting samples can be used in industrial applications respect to their high regenerability efficiency and high selectivity of the lead uptake from aqueous solutions.

Declaration of competing interest

The authors declare that they have no known competing financial interests or personal relationships that could have appeared to influence the work reported in this paper.

References

- Al Hamouz, O.C.S., Ali, S.A., 2012. Removal of heavy metal ions using a novel cross-linked polyzwitterionic phosphonate. *Sep. Purif. Technol.* 98, 94–101.
- Aldawsari, A., et al., 2022. Multiuse silicon hybrid polyurea-based polymer for highly effective removal of heavy metal ions from aqueous solution. *Int. J. Environ. Sci. Technol.* 19 (4), 2925–2938.
- Alimohammady, M., Jahangiri, M., Kiani, F., Tahermansouri, H., 2018. Competent heavy metal adsorption by modified MWNTs and optimization process by experimental design. *J. Environ. Eng.* 144 (11), 04018114.
- ALothman, Z.A., 2012. A review: fundamental aspects of silicate mesoporous materials. *Materials*, 5(12), 2874–2902.
- Badruddoza, A.Z.M., et al., 2013. Fe₃O₄/cyclodextrin polymer nanocomposites for selective heavy metals removal from industrial wastewater. *Carbohydr. Polym.* 91 (1), 322–332.
- Baraka, A., Hall, P., Heslop, M., 2007. Melamine–formaldehyde–NTA chelating gel resin: Synthesis, characterization and application for copper (II) ion removal from synthetic wastewater. *J. Hazard. Mater.* 140 (1–2), 86–94.
- Bashir, M.J., Aziz, H.A., Yusoff, M.S., Adlan, M.N., 2010. Application of response surface methodology (RSM) for optimization of ammoniacal nitrogen removal from semi-aerobic landfill leachate using ion exchange resin. *Desalination* 254 (1–3), 154–161.
- Bayo, J., 2012. Kinetic studies for Cd (II) biosorption from treated urban effluents by native grapefruit biomass (*Citrus paradisi* L.): The competitive effect of Pb (II), Cu (II) and Ni (II). *Chemical Engineering Journal*, 191, 278–287.
- Beamson, G., Briggs, D., 1992. *High resolution XPS of organic polymers*, Wiley.
- Castro-Muñoz, R., González-Melgoza, L.L., García-Depraect, O., 2021. Ongoing progress on novel nanocomposite membranes for the separation of heavy metals from contaminated water. *Chemosphere* 270, 129421.
- Chen, Q., et al., 2018. Comparison of heavy metal removals from aqueous solutions by chemical precipitation and characteristics of precipitates. *J. Water Process Eng.* 26, 289–300.
- Chen, X., Huang, G., Wang, J., 2013. Electrochemical reduction/oxidation in the treatment of heavy metal wastewater. *J. Metall. Eng. (ME)* 2 (4).
- Classen, T., et al., 2007. Hydrogen and coordination bonding supramolecular structures of trimesic acid on Cu (110). *Chem. A Eur. J.* 111 (49), 12589–12603.
- Cui, L., et al., 2020. Tetraphenylthene-based conjugated microporous polymer for aggregation-induced electrochemiluminescence. *ACS Appl. Mater. Interfaces* 12 (7), 7966–7973.
- Darvishi Cheshmeh Soltani, R., Safari, M., Rezaee, A., Godini, H., 2015. Application of a compound containing silica for removing ammonium in aqueous media. *Environ. Prog. Sustain. Energy*, 34(1), 105–111.
- Dizaj Khalili, A., Ghaemi, A., 2021. Utilization of response surface methodology, kinetic and thermodynamic studies on cadmium adsorption from aqueous solution by steel slag. *J. Iran. Chem. Soc.* 18 (11), 3031–3045.
- Ebrahimpour, E., Kazemi, A., 2023. Mercury (II) and lead (II) ions removal using a novel thiol-rich hydrogel adsorbent; PHPAm/Fe₃O₄@ SiO₂-SH polymer nanocomposite. *Environ. Sci. Pollut. Res.* 30 (5), 13605–13623.
- Ehgartner, C., et al., 2021. Carboxylic acid-modified polysilsesquioxane aerogels for the selective and reversible complexation of heavy metals and organic molecules. *Micropor. Mesopor. Mater.* 312, 110759.
- Fiyadh, S.S., et al., 2019. Review on heavy metal adsorption processes by carbon nanotubes. *J. Clean. Prod.* 230, 783–793.
- Ge, F., Li, M.-M., Ye, H., Zhao, B.-X., 2012. Effective removal of heavy metal ions Cd²⁺, Zn²⁺, Pb²⁺, Cu²⁺ from aqueous solution by polymer-modified magnetic nanoparticles. *J. Hazard. Mater.* 211, 366–372.
- Ghaemi, A., Mashhadimoslem, H., Zohourian Izadpanah, P., 2022. NiO and MgO/activated carbon as an efficient CO₂ adsorbent: characterization, modeling, and optimization. *Int. J. Environ. Sci. Technol.* 19 (2), 727–746.
- Gonte, R., Balasubramanian, K., 2016. Heavy and toxic metal uptake by mesoporous hypercrosslinked SMA beads: Isotherms and kinetics. *J. Saudi Chem. Soc.* 20, S579–S590.
- He, Y., et al., 2017. Efficient removal of Pb (II) by amine functionalized porous organic polymer through post-synthetic modification. *Sep. Purif. Technol.* 180, 142–148.
- Huang, J., 2009. Treatment of phenol and p-cresol in aqueous solution by adsorption using a carbonylated hypercrosslinked polymeric adsorbent. *J. Hazard. Mater.* 168 (2–3), 1028–1034.
- Huang, L., et al., 2021. Nanoarchitected porous organic polymers and their environmental applications for removal of toxic metal ions. *Chem. Eng. J.* 408, 127991.
- Hubiccki, Z., Kotodyńska, D., 2012. Selective removal of heavy metal ions from waters and waste waters using ion exchange methods. *Ion Exchange Technol.* 7, 193–240.
- James, A.M., et al., 2019. Selective environmental remediation of strontium and cesium using sulfonated hyper-cross-linked polymers (SHCPs). *ACS Appl. Mater. Interfaces* 11 (25), 22464–22473.
- Kim, S.-H., et al., 2020. Novel porous carbon material derived from hypercross-linked polymer of p-xylene for supercapacitors electrode. *Mater. Lett.* 263, 127222.
- Kim, B., Lim, S.-T., 1999. Removal of heavy metal ions from water by cross-linked carboxymethyl corn starch. *Carbohydr. Polym.* 39 (3), 217–223.
- Kong, X., Li, S., Strømme, M., Xu, C., 2019. Synthesis of porous organic polymers with tunable amine loadings for CO₂ capture: balanced physisorption and chemisorption. *Nanomaterials* 9 (7), 1020.
- Konstas, K., et al., 2012. Lithiated porous aromatic frameworks with exceptional gas storage capacity. *Angew. Chem.* 124 (27), 6743–6746.
- Li, B., et al., 2011. A new strategy to microporous polymers: knitting rigid aromatic building blocks by external cross-linker. *Macromolecules* 44 (8), 2410–2414.
- Li, B., et al., 2011. Hypercrosslinked microporous polymer networks for effective removal of toxic metal ions from water. *Microporous Mesoporous Mater.* 138 (1–3), 207–214.
- Li, X., et al., 2015. Studies of heavy metal ion adsorption on Chitosan/Sulfhydryl-functionalized graphene oxide composites. *J. Colloid Interface Sci.* 448, 389–397.
- Li, Y., et al., 2017. Post-synthesis modification of porous organic polymers with amine: a task-specific microenvironment for CO₂ capture. *Int. J. Coal Sci. Technol.* 4 (1), 50–59.
- Li, J., et al., 2018. Metal-organic framework-based materials: superior adsorbents for the capture of toxic and radioactive metal ions. *Chem. Soc. Rev.* 47 (7), 2322–2356.
- Liu, T., et al., 2023. Recent developments in the utilization of modified graphene oxide to adsorb dyes from water: A review. *J. Ind. Eng. Chem.* 117, 21–37.
- Lu, X.-F., et al., 2019. Preparation of carboxy-functionalized organic framework for efficient removal of Hg²⁺ and Pb²⁺ from water. *Ind. Eng. Chem. Res.* 58 (38), 17660–17667.
- Maleki, F., Ghaemi, A., G. Mir Mohamad Sadeghi, 2022. Synthesis and characterization of waste Styrofoam hypercrosslinked polymer as an adsorbent for CO₂ capture. *Environmental Progress & Sustainable Energy*, e13954.
- Manakhov, A.M., et al., 2023. Immobilization and release of platelet-rich plasma from modified nanofibers studied by advanced X-ray photoelectron spectroscopy analyses. *Polymers* 15 (6), 1440.
- Mashhadimoslem, H., et al., 2021. Biomass derived hierarchical porous carbon for high-performance O₂/N₂ adsorption; a new green self-activation approach. *RSC Adv.* 11 (57), 36125–36142.
- Masoumi, H., Ghaemi, A., Gilani, H.G., 2021. Evaluation of hyper-cross-linked polymers performances in the removal of hazardous heavy metal ions: A review. *Sep. Purif. Technol.* 260, 118221.
- Masoumi, H., Ghaemi, A., Gilani, H.G., 2021. Exploiting the performance of hyper-cross-linked polystyrene for removal of multi-component heavy metal ions from wastewaters. *J. Environ. Chem. Eng.* 9 (4), 105724.
- Masoumi, H., Ghaemi, A., Gilani, H.G., 2021. Synthesis of polystyrene-based hyper-cross-linked polymers for Cd (II) ions removal from aqueous solutions: Experimental and RSM modeling. *J. Hazard. Mater.* 416, 125923.
- Masoumi, H., Ghaemi, A., Ghanadzadeh, H.G., 2021. Elimination of lead from multi-component lead-nickel-cadmium solution using hyper-cross-linked polystyrene: Experimental and RSM modeling. *J. Environ. Chem. Eng.* 9 (6), 106579.
- Monier, M., Ayad, D., Abdel-Latif, D., 2012. Adsorption of Cu (II), Cd (II) and Ni (II) ions by cross-linked magnetic chitosan-2-aminopyridine glyoxal Schiff's base. *Colloids Surf. B Biointerfaces* 94, 250–258.
- Moradi, M.R., Ramezani-pour Penchah, H., Ghaemi, A. CO₂ capture by Benzene-Based Hypercrosslinked Polymer adsorbent: artificial neural network and response surface methodology. *The Canadian Journal of Chemical Engineering*.
- Mu, Z., et al., 2022. Covalent Organic Frameworks with Record Pore Apertures. *J. Am. Chem. Soc.* 144 (11), 5145–5154.
- Özsin, G., Kılıç, M., Apaydın-Varol, E., Pütün, A.E., 2019. Chemically activated carbon production from agricultural waste of chickpea and its application for heavy metal adsorption: equilibrium, kinetic, and thermodynamic studies. *Appl. Water Sci.* 9 (3), 1–14.
- Panayotova, M., Velikov, B., 2003. Influence of zeolite transformation in a homoionic form on the removal of some heavy metal ions from wastewater. *J. Environ. Sci. Health A* 38 (3), 545–554.
- Qin, X., et al., 2019. β-Cyclodextrin-crosslinked polymeric adsorbent for simultaneous removal and stepwise recovery of organic dyes and heavy metal ions: fabrication, performance and mechanisms. *Chem. Eng. J.* 372, 1007–1018.
- Ramezani-pour Penchah, H., Ghaemi, A., Ganadzadeh Gilani, H., 2019. Benzene-based hyper-cross-linked polymer with enhanced adsorption capacity for CO₂ capture. *Energy Fuel* 33 (12), 12578–12586.
- Sang, Y., Shao, L., Huang, J., 2020. Carbonyl functionalized hyper-cross-linked polymers for CO₂ capture. *J. Polym. Res.* 27, 1–8.
- Sel, K., et al., 2015. Benign preparation of metal-organic frameworks of trimesic acid and Cu, Co or Ni for potential sensor applications. *J. Electron. Mater.* 44, 136–143.
- Shih, Y.-J., Chien, S.-K., Jhang, S.-R., Lin, Y.-C., 2019. Chemical leaching, precipitation and solvent extraction for sequential separation of valuable metals in cathode material of spent lithium ion batteries. *J. Taiwan Inst. Chem. Eng.* 100, 151–159.
- Singh, S., et al., 2023. Graphene oxide-based novel MOF nanohybrid for synergic removal of Pb (II) ions from aqueous solutions: Simulation and adsorption studies. *Environ. Res.* 216, 114750.
- Song, S., et al., 2021. Synthesis of carboxyl-modified hyper-cross-linked polymers with conspicuous removal capability for various water-soluble contaminants. *J. Environ. Chem. Eng.* 9 (5), 106047.
- Sun, Y., et al., 2020. Flocculation activity and evaluation of chitosan-based flocculant CMCTS-gP (AM-CA) for heavy metal removal. *Sep. Purif. Technol.* 241, 116737.

- Taha, A., Shreadah, M.A., Ahmed, A., Heiba, H.F., 2016. Multi-component adsorption of Pb (II), Cd (II), and Ni (II) onto Egyptian Na-activated bentonite; equilibrium, kinetics, thermodynamics, and application for seawater desalination. *J. Environ. Chem. Eng.* 4 (1), 1166–1180.
- Tahermansouri, H., Beheshti, M., 2013. Kinetic and equilibrium study of lead (II) removal by functionalized multiwalled carbon nanotubes with isatin derivative from aqueous solutions. *Bull. Kor. Chem. Soc.* 34 (11), 3391–3398.
- Ubando, A.T., et al., 2021. Microalgal biosorption of heavy metals: a comprehensive bibliometric review. *J. Hazard. Mater.* 402, 123431.
- Vakili, M., et al., 2019. Regeneration of chitosan-based adsorbents used in heavy metal adsorption: A review. *Sep. Purif. Technol.* 224, 373–387.
- Verma, M., et al., 2022. Multifunctional β -Cyclodextrin-EDTA-Chitosan polymer adsorbent synthesis for simultaneous removal of heavy metals and organic dyes from wastewater. *Environ. Pollut.* 292, 118447.
- Vogel, A.I., Furniss, B.S., 1978. *Vogel's Practical organic chemistry, including qualitative organic analysis*, Longman.
- Wang, H., et al., 2019. Covalent triazine frameworks for carbon dioxide capture. *J. Mater. Chem. A* 7 (40), 22848–22870.
- Wang, R.-D., et al., 2022. A novel dual-functional coordination polymer for detection and ultra-effectively removal of Fe (III) in water. *J. Mol. Liq.* 355, 118942.
- Wang, Q., Li, R., Ouyang, X., Wang, G., 2019. A novel indole-based conjugated microporous polymer for highly effective removal of heavy metals from aqueous solution via double cation- π interactions. *RSC Adv.* 9 (69), 40531–40535.
- Wang, J., Liu, F., 2014. Enhanced and selective adsorption of heavy metal ions on ion-imprinted simultaneous interpenetrating network hydrogels. *Des. Monomers Polym.* 17 (1), 19–25.
- Wei, Y., Parmentier, T.E., de Jong, K.P., Zečević, J., 2015. Tailoring and visualizing the pore architecture of hierarchical zeolites. *Chem. Soc. Rev.* 44 (20), 7234–7261.
- Wu, W., et al., 2013. Highly efficient removal of Cu (II) from aqueous solution by using graphene oxide. *Water Air Soil Pollut.* 224, 1–8.
- Yang, Z., et al., 2021. Removal of various pollutants from wastewaters using an efficient and degradable hypercrosslinked polymer. *Sep. Sci. Technol.* 56 (5), 860–869.
- Yang, Z., Huang, X., Yao, X., Ji, H., 2018. Thiourea modified hyper-crosslinked polystyrene resin for heavy metal ions removal from aqueous solutions. *J. Appl. Polym. Sci.* 135 (1), 45568.
- Yilmaz, S.S., et al., 2007. Synthesis of a novel crosslinked superabsorbent copolymer with diazacyclooctadecane crown ether and its sorption capability. *Eur. Polym. J.* 43 (5), 1923–1932.
- Yuan, S., et al., 2018. Stable metal-organic frameworks: design, synthesis, and applications. *Adv. Mater.* 30 (37), 1704303.
- Zaferani, S.P.G., Emami, M.R.S., Amiri, M.K., Binaeian, E., 2019. Optimization of the removal Pb (II) and its Gibbs free energy by thiosemicarbazide modified chitosan using RSM and ANN modeling. *Int. J. Biol. Macromol.* 139, 307–319.
- Zare-Dorabei, R., Ferdowsi, S.M., Barzin, A., Tadjarodi, A., 2016. Highly efficient simultaneous ultrasonic-assisted adsorption of Pb (II), Cd (II), Ni (II) and Cu (II) ions from aqueous solutions by graphene oxide modified with 2, 2'-dipyridylamine: central composite design optimization. *Ultrason. Sonochem.* 32, 265–276.
- Zeng, L., et al., 2015. Adsorption of Cd (II), Cu (II) and Ni (II) ions by cross-linking chitosan/rectorite nano-hybrid composite microspheres. *Carbohydr. Polym.* 130, 333–343.
- Zhang, W., et al., 2013. A photoelectron spectroscopy study on the interfacial structure and electronic structure of terephthalic acid adsorption on TiO₂ (110)-(1 \times 1) surface. *J. Phys. Chem. C* 117 (41), 21351–21358.
- Zhang, Y., Chen, Y., Wang, C., Wei, Y., 2014. Immobilization of 5-aminopyridine-2-tetrazole on cross-linked polystyrene for the preparation of a new adsorbent to remove heavy metal ions from aqueous solution. *J. Hazard. Mater.* 276, 129–137.
- Zhou, H., et al., 2022. Enhancement of performance and stability of thin-film nanocomposite membranes for organic solvent nanofiltration using hypercrosslinked polymer additives. *J. Membr. Sci.* 644, 120172.
- Zhu, J.-H., et al., 2014. Preparation and adsorption performance of cross-linked porous polycarbazoles. *J. Mater. Chem. A* 2 (38), 16181–16189.